frontiers | Frontiers in Marine Science

TYPE Original Research
PUBLISHED 26 October 2022
DOI 10.3389/fmars.2022.1017052

OPEN ACCESS

EDITED BY
Kostas Kiriakoulakis,
Liverpool John Moores University,
United Kingdom

REVIEWED BY
Manuel Vargas-Yáñez,
Spanish Institute of Oceanography (IEO), Spain
Mauro Celussi,
Istituto Nazionale di Oceanografia e di Geofisica Sperimentale, Italy

*CORRESPONDENCE
Sarah Paradis
sparadis@ethz.ch

SPECIALTY SECTION
This article was submitted to Deep-Sea Environments and Ecology, a section of the journal Frontiers in Marine Science

RECEIVED 11 August 2022
ACCEPTED 28 September 2022
PUBLISHED 26 October 2022

CITATION
Paradis S, Arjona-Camas M, Goñi M, Palanques A, Masqué P and Puig P (2022) Contrasting particle fluxes and composition in a submarine canyon affected by natural sediment transport events and bottom trawling. *Front. Mar. Sci.* 9:1017052. doi: 10.3389/fmars.2022.1017052

Contrasting particle fluxes and composition in a submarine canyon affected by natural sediment transport events and bottom trawling

Sarah Paradis[1,2,3]*, Marta Arjona-Camas[2], Miguel Goñi[4], Albert Palanques[2], Pere Masqué[1,5,6] and Pere Puig[2]

[1]Institute of Environmental Science and Technology (ICTA), Universitat Autònoma de Barcelona, Bellaterra, Spain, [2]Marine Sciences Institute, Consejo Superior de Investigaciones Científicas (ICM-CSIC), Barcelona, Spain, [3]Geological Institute, Department of Earth Sciences, Eidgenössische Technische Hochschule (ETH) Zürich, Zürich, Switzerland, [4]College of Earth, Ocean, and Atmospheric Sciences, Oregon State University, Corvallis, OR, United States, [5]School of Natural Sciences, Centre for Marine Ecosystems Research, Edith Cowan University, Joondalup, WA, Australia, [6]Marine Environment Laboratories, International Atomic Energy, Principality of Monaco, Monaco

Submarine canyons are important conduits of sediment and organic matter to deep-sea environments, mainly during high-energy natural events such as storms, river floods, or dense shelf water cascading, but also due to human activities such as bottom trawling. The contributions of natural and trawling-induced sediment and organic matter inputs into Palamós Canyon (NW Mediterranean) were assessed from three instrumented moorings deployed in the axis and northern flank of the canyon covering the trawling closure (February) and the trawling season (March-December) of 2017. During the trawling closure, large sediment fluxes with high contents of labile marine organic matter content were registered in the canyon axis, associated to storm resuspension on the shelf that coincided with dense shelf water cascading and high surface water productivity. Although no major natural sediment transport events occurred during the following spring and summer months, near-daily trawling-induced sediment gravity flows were recorded in the northern flank mooring, placed directly below a fishing ground, which sometimes reached the canyon axis. Compositionally, the organic matter transferred by trawling resuspension was impoverished in the most labile biomarkers (fatty acids, amino acids, and dicarboxylic acids) and had a high degree of degradation, which was similar to surficial sediment from the adjacent fishing ground. Trawling resuspended particles masked the transfer of organic matter enriched in labile biomarkers that naturally occur during the quiescent

summer months. Overall, bottom trawling enhances the magnitude of particle fluxes while modifying its organic carbon composition, increasing the re-exposure and transfer of degraded organic carbon and potentially affecting benthic communities that rely on the arrival of fresh organic matter.

KEYWORDS

submarine canyon, NW Mediterranean, surface sediment, sediment transport, carbon cycle, biomarkers, storms, bottom trawling

1 Introduction

Submarine canyons act as preferential conduits of particulate matter connecting the productive coastal shelf with the nutrient-limited abyss (Allen and Durrieu de Madron, 2009; Puig et al., 2014; Porter et al., 2016). The enhanced flux of organic matter into canyons combined with their heterogenous set of habitats makes these morphological features important nursery and refuge areas for diverse marine life (Vetter et al., 2010; De Leo et al., 2014; Fernandez-Arcaya et al., 2017). Consequently, several benthic species of commercial interest tend to congregate near submarine canyons, supporting many fishing grounds (Farrugio, 2012).

The ecological importance of submarine canyons relies on the transfer of organic matter to the canyon's interior, which is enhanced by natural processes that increase the flux of particulate matter into canyons (see review by Puig et al., 2014). These processes include river floods that deliver elevated amounts of suspended sediment to the margin and high-energy storm-waves, which resuspend sediment from shallower regions of the shelf. Combined, both processes can transport elevated amounts of suspended particulate matter into canyons as turbidity currents and/or hyperpycnal flows (Martín et al., 2011; Liu et al., 2012; Puig et al., 2014). Dense shelf water cascading (DSWC) events generated by cooling and/or evaporation of coastal surface waters can also transport large amounts of particulate matter into canyons. Their excess in density forces these waters to sink to greater depths through submarine canyons as gravity-driven currents that carry resuspended sediment until reaching neutral buoyancy (Durrieu de Madron et al., 2005; Canals et al., 2006; Palanques et al., 2012). Particulate fluxes derived from both storms and DSWC tend to be highest in the upper and middle canyon reaches, and decrease with depth as the hydrodynamic forces subside, rarely reaching the lower canyon (de Stigter et al., 2007; Palanques et al., 2012; Pedrosa-Pàmies et al., 2013). Sediment transported during storms and DSWC generally have relatively low particulate organic matter content and is composed of aged terrestrial organic carbon (OC) eroded from the continental shelf (Sanchez-Vidal et al., 2008; Tesi et al., 2010; Martín et al., 2011; Hsu et al., 2014; Sparkes et al., 2015). However, when these events occur in coincidence with phytoplankton blooms, particulate matter enriched with marine OC is transferred into submarine canyons (Fabres et al., 2008; Pasqual et al., 2010; Lopez-Fernandez et al., 2013a).

Anthropogenic activities can also modify the transport of sediment in submarine canyons. Several studies have proven that deep bottom trawling around submarine canyons can be a main driver of particulate matter transfer (Martín et al., 2006; Palanques et al., 2006; Puig et al., 2012; Martín et al., 2014a; Wilson et al., 2015; Arjona-Camas et al., 2019; 2021). This enhanced transferal of particulate matter has caused a general increase in sedimentation rates within the axes of several trawled submarine canyons (Martín et al., 2008; Puig et al., 2015; Paradis et al., 2017; 2018a; 2018b; 2021a), which has modified the abundance and biodiversity of meiobenthos (Pusceddu et al., 2014; Román et al., 2018). These shifts in meiobenthic community structures are attributed to a presumed alteration in both the amount and the composition of organic matter transferred into canyons, since bottom sediments from fishing grounds tend to be depleted in labile organic matter compounds (Martín et al., 2014b; Pusceddu et al., 2014; Paradis et al., 2021b) and the organic matter associated with local resuspended sediment tends to be highly degraded (Pusceddu et al., 2015; Wilson et al., 2015; Wu et al., 2016; Daly et al., 2018). However, the organic matter composition of downward particulate matter transferred antropogenically from fishing grounds into canyon axes have not been studied yet.

The NW Mediterranean margin is incised by several canyons that present large particle fluxes from both natural sediment transport processes and from bottom trawling activities, and Palamós Canyon (also known as La Fonera Canyon) is one of the most prominent of these. Northern storms are frequent and persistent in this margin, but they generate relatively small waves (~2 m) on the inner shelf that have limited capacity to resuspend sediment. In contrast, the rarer eastern storms generally present larger waves (> 4 m) and are accompanied by heavy rains and torrential river discharges carrying large amounts of sediment to the coast. In the case of Palamós Canyon, the Ter River is the closest to its canyon head and contributes significant amounts of terrigenous material to the system (Palanques et al., 2005). These eastern storms also resuspend sediments that are then intercepted by Palamós Canyon, supplying large amounts of OC-poor sediment into the canyon (Martín et al., 2006). DSWC in the NW Mediterranean margin originates in the Gulf of Lions during winter and generates a southward flow of cold dense water that reaches Palamós Canyon in

specific years, supplying large amounts of sediment into it (Ribó et al., 2011; Arjona-Camas et al., 2021).

Palamós Canyon supports important trawling grounds along its northern and southern flanks, named Sant Sebastià and Rostoll fishing grounds, respectively (Figure 1). These fishing grounds are concentrated at the 400-800 m depth range in accordance to the life-cycle of their most targeted commercial species, the highly coveted red-and-blue deep-sea shrimp *Aristeus antennatus* (Sardà et al., 1994; Tudela et al., 2003). Chronic bottom trawling activities along the canyon's flanks cause almost daily sediment resuspension evolving into gravity flows towards the canyon's interior (Palanques et al., 2006; Puig et al., 2012; Martín et al., 2014b), which can be detached as persistent nepheloid layers at the same depth range of the fishing grounds (Martín et al., 2014b; Arjona-Camas et al., 2021). Trawling-derived sediment gravity flows are then channeled through canyon flank tributaries, such as the Montgrí gully in the northern flank (Figure 1), and can reach the canyon axis, transporting eroded sediment with high silt content, as well as lower OC and opal content (Martín et al., 2006; Palanques et al., 2006). However, these studies have not assessed the variations in the composition of downward particulate organic matter transported by natural and trawling activities.

Hence, the aim of this study is to evaluate how sediment transport events linked to both natural processes and trawling activities influence the composition of downward particulate organic matter into Palamós Canyon, using biomarkers yielded from the oxidation of CuO which have been used to assess the origin and degree of degradation of organic matter transferred into canyons (Tesi et al., 2008; Goñi et al., 2013; Pasqual et al., 2010; 2013). To address this, three instrumented moorings were deployed in Palamós Canyon to measure the sedimentary dynamics and the downward particle fluxes and their composition from February to December 2017. Since 2013, a two-month trawling closure occurs in Palamós Canyon from early January to early March to allow the recruitment of shrimp juveniles and avoid the risk of overexploitation of the fishing stock (Bjørkan et al., 2020), providing a time-window to study natural particle fluxes in February and the effect of trawling activities for the remainder of the year. To identify the alteration of organic matter compounds transferred into the canyon by natural sediment transport processes and bottom trawling activities, we compared the sedimentological and biogeochemical composition of sediment trap samples along with the composition of surface sediment obtained on the adjacent trawling grounds.

2 Materials and methods

2.1 Fieldwork and instrumentation

To conduct this observational study, three moorings were deployed in Palamós Canyon: at 929 m water depth in the canyon axis (Axis-900), at 975 m water depth in the Montgrí tributary gully located ~0.5 km from Sant Sebastià trawling ground (Flank-1000), and at 1230 m water depth in the confluence of the tributary gully and the canyon axis, at ~2 km from the same fishing ground (Axis-1200), and ~4 km down-canyon from Axis-900 mooring (Figure 1). The moorings were deployed in three consecutive periods: from February 7 to June 5 and from June 9 to October 3 2017, and from October 3 2017 to March 5 2018, but this study was centered on data of 2017 (Figure S1).

Mooring Axis-900 was equipped with an autonomous hydrographic profiler (Aqualog), as well as a near-bottom autonomous turbidimeter (AQUA-logger 210TY) with a SeaPoint turbidity sensor set to record turbidity in Formazin Turbidity Unit (FTU) at 1-min intervals in auto-gain mode, placed at 5 m above the bottom (mab), and a current meter (Aquadopp, Nortek) coupled with a temperature sensor (SeaBird SBE-37) set to record at 5-min intervals and placed at 6 mab. The Aqualog only registered data from February 7 to April 7, and the results are explained in detail in Arjona-Camas et al. (2021). The current meter stopped some days before the end of the first and second deployments acquiring data from February 7 to May 20 and from June 9 to September 8, respectively, whereas it recorded data during all of the third deployment (Figure S1).

Mooring Flank-1000 had a string of 5 single-point autonomous turbidimeters (AQUA logger 210TY, AQUATEC) placed at 5, 10, 20, 50 and 80 mab, each one equipped with temperature, pressure, and a SeaPoint turbidity sensor set to record FTUs at 1-min sampling interval. The mooring line also held a downward-looking 300 kHz Teledyne RDI Acoustic Doppler Current Profiler (ADCP) placed above the turbidimeters, which provided current velocity and direction from 10 to 80 mab in 2-m bins at 5-min intervals. The turbidimeter at 20 mab from the first deployment presented increasing FTUs over time, indicating the effect of biofouling. Hence, data from this sensor were omitted (Figure S1).

Mooring Axis-1200 was equipped with a single-point autonomous turbidimeter (AQUA logger 210TY, AQUATEC) set to record at 1-min intervals in auto-gain mode, placed at 5 mab, and a current meter (Aquadopp, Nortek) paired with a conductivity and temperature sensor (SeaBird SBE-37) and a SeaPoint turbidimeter (0-25 FTU) set to record at 5-min intervals placed at 6 mab. The autonomous turbidity sensor of the first deployment did not work, so the turbidity data were extracted from the turbidimeter paired with the current meter, providing values up to 25 FTUs. Unfortunately, the current meter only acquired data from February 7 to March 21 and from June 6 to October 3 (Figure S1). Additionally, this mooring had a 24-cup sediment trap Technicap PPS3/3 model, with a 0.125 m^2 cylindrical opening and an aspect ratio of 2.5 (1 m long/0.4 m wide), placed at 22 mab and programmed to collect downward particulate fluxes at 7-day intervals, from Monday to Sunday, to assess the weekly particle fluxes. The sediment trap overfilled in

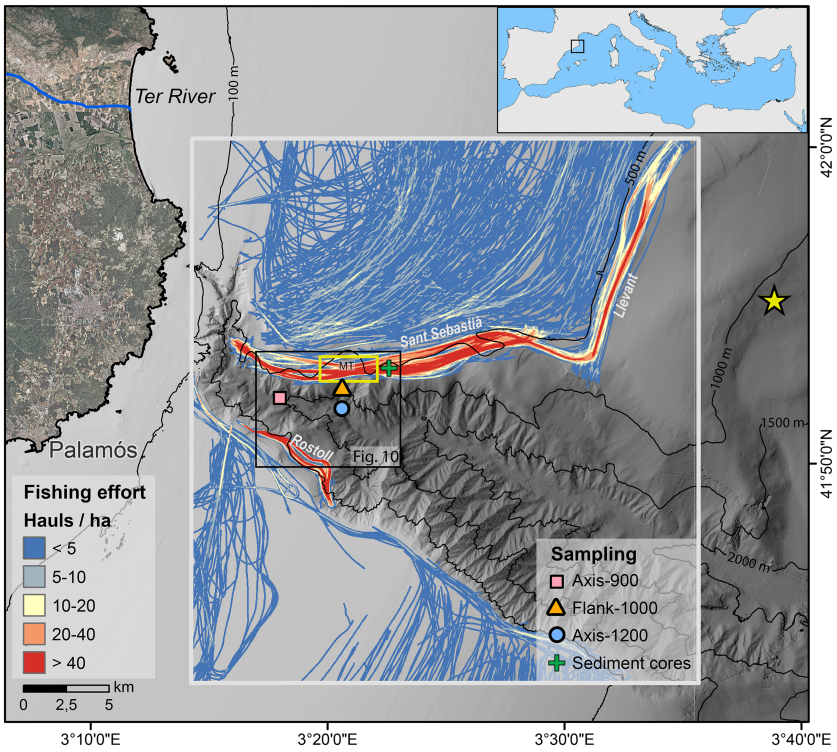

FIGURE 1
Bathymetric map of Palamós Canyon, with the location of Axis-900 (pink square) mooring at the canyon axis, Flank-1000 mooring (orange triangle) deployed in the Montgrí tributary gully (MT) and Axis-1200 mooring (blue circle) deployed in the confluence between MT and the canyon axis. The yellow rectangle above the Flank-1000 mooring delimits the section of the fishing ground where daily hauls were extracted for Figure 2. Composition of the sediment trap (Axis-1200) was compared with surficial composition of the sediment core collected in the trawled flank (green cross). Fishing effort is given as cumulative number of hauls per hectare obtained from AIS data from February to December 2017, identifying the main fishing grounds (Sant Sebastià, Rostoll, Llevant). The location of the Cap Begur buoy is given by a yellow star.

the 4th sample of the first deployment (March 6-13) and in the 8th sample of the third deployment (December 4-11), providing valid samples only from February 13 to March 9 and from June 12 to December 7 (Figure S1).

Current speeds and directions from the different current meters were decomposed in E-W and N-S current velocity components. In order to obtain the along- and across-canyon directions for the Axis-900 and Axis-1200 moorings, data from these moorings were rotated 70° clockwise to align their reference frames to the canyon axis orientation, converting the N-S velocity component into the along-canyon velocity component (positive up-canyon) and the E-W velocity component into the across-canyon velocity component (positive towards the NNE). Data of the Flank-1000 mooring were rotated 11° counterclockwise to align the reference frame to the canyon gully orientation, converting the N-S velocity component into the along-gully velocity component (positive up-gully), and the E-W velocity component into the across-gully velocity component (positive towards ESE). To make the three moorings comparable among them, all current direction components were reported with respect to the main canyon axis orientation: along-canyon (i.e. across-gully for Flank-1000) and across-canyon (i.e. along-gully for Flank-1000). FTUs from the different turbidimeters were converted to estimates of suspended sediment concentration (SSC; mg·L^{-1}) following the calibration described in Arjona-Camas et al. (2021). Cumulative sediment transport (kg·m^{-2}) in the across- and along-canyon direction were calculated through the cumulative sum of the product of the decomposed and rotated current speed and the SSC. Given the maximum acquisition of turbidity values of Axis-1200 in the first deployment and the missing data between mooring deployments, cumulative suspended sediment transport must be regarded as lower estimates.

In addition, three sediment cores were taken on the trawled northern flank of Palamós Canyon (Figure 1), at the time of the first deployment and during the mooring turnaround cruises: one during the temporal trawling close season in February 7, and two during the trawling season, in June 5 and in October 3. The cores were collected using a K/C Denmark multicorer at ~500-m depth (see Paradis et al. (2021b) for further details).

2.2 Sediment sample treatment and analytical procedure

Sediment trap samples were prepared and processed in the laboratory using the same method as described in Palanques and Puig (2018), obtaining sub-sample aliquots for each sample. Total mass flux (TMF; $g \cdot m^{-2} \cdot d^{-1}$) was calculated from the sample dry weight of two sub-sample aliquots, which were averaged and upscaled based on their dilution factor, and divided by the collecting area (0.125 m^2) and the sampling interval (7 days) of the sediment trap, with an average standard error of 2.4%.

Average grain size and the fraction of clay (< 4 μm), silt (4 – 63 μm), and sand (63 μm – 2 mm) in downward particulate fluxes were analyzed using a Horiba Partica LA-950 V2m particle-size analyzer by oxidizing approximately 1 g of sample using 20% H_2O_2 and disaggregating with 2.5% $P_2O_7^{4-}$.

Elemental analysis of total carbon (TC), organic carbon (OC) and total nitrogen (TN) contents were carried out with an elemental analyzer (Costech ECS Analyzer 4010), according to the procedure described by Nieuwenhuize et al. (1994). Prior to OC analysis, samples were first decarbonated through acid-fuming in the presence of 12 N HCl during 24 h and repeatedly adding 100 μL of 2 N HCl to the sample until effervescence ceased. Inorganic carbon, quantified as the difference between total carbon and organic carbon, was converted to $CaCO_3$ contents using the molecular mass ratio of 100/12, assuming all inorganic carbon present is in the form of $CaCO_3$. Opal (biogenic silica) was analyzed using a wet-alkaline extraction with sodium carbonate using the method described by Mortlock and Froelich (1989). Finally, the lithogenic fraction was calculated as the difference between the total mass and the main mass constituents ($CaCO_3$, organic matter, and opal), where organic matter content was estimated as twice the OC content.

Specific biomarkers yielded from the CuO oxidation of sediment trap samples were analyzed following the method described by Goñi and Montgomery (2000). Briefly, between 250 and 400 mg of homogenized ground sample was oxidized with CuO under basic conditions (2 N NaOH) in an oxygen-free atmosphere at 150°C for 90 min in a microwave. After oxidation, samples were spiked with ethyl vanillin and trans-cinnamic acid as recovery standards, after which the samples were acidified to 1 pH using small volumes of concentrated HCl, and subsequently extracted twice using ethyl acetate. Samples were then evaporated under a constant flow of nitrogen gas, reconditioned in pyridine, and derivatized by adding bistrimethylsilyltrifluoroacetamide (BSTFA) + 10% trimethylchlorosilane (TMCS). Specific reaction products (Table S1) were quantified by GC-MS (Hewlett Packard 6890 GC System) with DB1 column and the HP5973 mass selective detector through selective ion monitoring as previously described by Goni et al. (2009). CuO yields were grouped into specific compound classes that have distinct chemical precursors including those from specific terrestrial sources such as vascular plants (lignin phenols, cutin acids, and certain p-hydroxybenzenes), soil (certain benzoic acids), as well as compound classes (fatty-acids, di-carboxylic acids, amino acids) that can be of both marine and terrestrial origin (Table S1). Mean concentrations of the parameters were calculated as flux-weighted mean concentrations over the whole sampling period, as explained by Heussner et al. (1990).

Sediment samples from the sediment cores taken on the trawled northern flank of Palamós Canyon during the cruises were analyzed for grain size, OC, TN, $CaCO_3$, and CuO biomarkers, following the same procedure as the sediment trap samples. The procedures and the results of these analysis were published in Paradis et al. (2021b). For this study we use the results of the surface sediment samples (0-1 cm) of these cores to compare them with the results of the sediment trap samples.

2.3 Forcing conditions

Significant wave height (H_s) was obtained from the Cap de Begur buoy (3.65° E, 41.92° N), located ~10 km NE at the continental slope region next to Palamós Canyon (Figure 1), which is managed by the Spanish Ports Authority. Storms were defined as H_s greater than 2 m for more than 6 h (Mendoza and Jiménez, 2009) and eastern storms were identified when the wave direction was between 60° and 120°. Daily Ter River discharge was obtained from the Catalan Water Agency. Data of net primary productivity (NPP) were extracted from the Ocean Productivity database (http://www.science.oregonstate.edu/ocean.productivity/index.php). NPP data from this database are calculated using the Vertically Generalized Production Model, which uses both surface chlorophyll concentrations and sea surface temperature data extracted from satellite imagery (Behrenfeld and Falkowski, 1997).

Trawling activity was obtained from vessel Automatic Identification System (AIS) extracted from Shiplocus, the official Spanish Port System module that manages and evaluates maritime traffic data. AIS data were filtered following the method described by Paradis et al. (2021b) to obtain the number of hauls per hectare in each fishing ground. The number of hauls above Montgrí tributary gully was then extracted from the polygon delimited in Figure 1.

2.4 Statistical analyses

Principal Component Analysis (PCA) was performed on CuO biomarkers of downward particulate fluxes obtained from the sediment trap (Axis-1200) to reduce the dimensions of the dataset and maximize the variance between samples. PCA was performed using Python's Scikit-learn module (Pedregosa et al., 2011) by first normalizing the data. Based on this PCA, PC loadings of OC composition of surface sediment collected in the adjacent

trawling ground (Paradis et al., 2021b) were used to study its relationship with the composition of downward particulate fluxes.

3 Results

3.1 Forcing conditions

During the sampling period, natural forcing conditions (H_s, Ter River discharge, and NPP) followed a similar seasonal pattern, with generally stronger events occurring during the winter (January-March) and autumn (October-December) months (Figures 2A–C). Although the majority of the storms were caused by northern winds, exceptionally strong eastern storms occurred in January 19-23 and in February 12-15 with H_s reaching 6 m and 5 m respectively, and strong Ter River floods, reaching 133 $m^3 \cdot s^{-1}$ and 30 $m^3 \cdot s^{-1}$ respectively during each eastern storm (Figures 2A, B). Although NPP also followed this general seasonal pattern, values were low during the first eastern storm in January (550 mg $C \cdot m^{-2} \cdot d^{-1}$) but increased during the second eastern storm in February due to a late-winter phytoplankton bloom (1200 mg $C \cdot m^{-2} \cdot d^{-1}$) (Figure 2C).

During the more quiescent late-spring and summer months, these natural forcing conditions receded to background values (~1 m H_s, ~3 $m^3 \cdot s^{-1}$ Ter River discharge, and ~450 mg $C \cdot m^{-2} \cdot d^{-1}$ NPP) (Figures 2A–C). The general decrease of NPP was interrupted by a second phytoplankton bloom in early-June (870 mg $C \cdot m^{-2} \cdot d^{-1}$) (Figure 2C).

From October to December, H_s increased again due to seasonal autumn storms (Figure 2A). These events were generally dry storms caused by northern winds that did not lead to significant increases in Ter River discharges (Figures 2A, B). NPP steadily increased during autumn until reaching ~780 mg $C \cdot m^{-2} \cdot d^{-1}$ in late-November and decreased again to background values in the following winter months (Figure 2C).

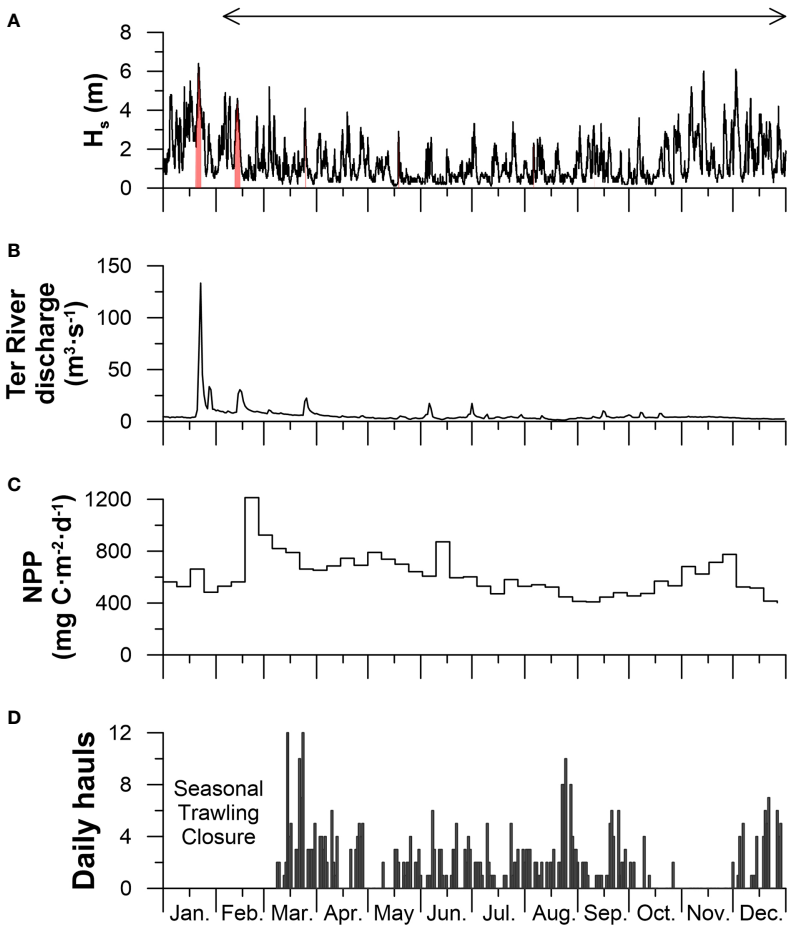

FIGURE 2
Forcing conditions in 2017. **(A)** Significant wave height (H_s) measured at the Cap de Begur buoy, where eastern storms are identified in red. **(B)** Ter River discharge. **(C)** 8-day average net primary productivity (NPP). **(D)** Daily hauls in the trawling ground above the Montgrí tributary gully (see yellow polygon in Figure 1). The horizontal arrow on top indicates the monitoring period.

Trawling effort in the Sant Sebastià fishing ground above the Montgrí tributary gully varied throughout the year (Figure 2D). No hauls were detected at the beginning of the year during the seasonal trawling closure, nor during the weekends or national holidays, when trawlers are not allowed to operate (Bjørkan et al., 2020). During working days, an average of 2 hauls per day were recorded, but trawling effort varied from 0 to 12 hauls per working day. Highest fishing effort occurred at the beginning of the trawling season in March, in late August, and again in late December, with 7 to 12 hauls per day (Figure 2D). During late October and throughout November, there was negligible trawling activity on the Sant Sebastià fishing ground (Figure 2D) since bottom trawlers had moved to shallower fishing grounds on the open slope (Figure S2).

3.2 Sediment transport in canyon axis (929 m water depth)

The time series of the Axis-900 mooring located in the canyon axis are presented in detail in Arjona-Camas et al. (2021), but described here briefly to contextualize the observed downward particle fluxes. Temperature recorded at 6 mab fluctuated between 13.2 and 13.6°C throughout the year, with a sharp drop to 12.6°C between February 13 and 15 (Figure 3A) due to an eastern storm concurrent with a DSWC event that caused a maximum peak in SSC of ~230 mg·L^{-1}. This event was initially directed down-canyon at 0.3 m·s^{-1}, but was followed by a quick up-canyon reversal of current direction reaching maximum values of 0.6 m·s^{-1} (Figure 3D), following the predominant up-canyon bottom current direction (~280°) at this site (Figure 3E).

Since the onset of trawling activities in March, several sporadic peaks of ~20 mg·L^{-1} were recorded only during weekdays, with exceptionally higher SSC of 190, 140, and 120 mg·L^{-1} at the end of July, in mid-August and at the end of September (Figure 3B). SSC was negligible during November, but small peaks of SSC (~60 mg·L^{-1}) resumed again in mid-December (Figure 3B). Current velocities presented fluctuating up-canyon and down-canyon flows (~0.15 m·s^{-1}), with increasing speeds of up to 0.4 m·s^{-1} towards the end of the year in November and December (Figure 3D). The predominant direction of near-bottom currents was up-canyon (~280°), although currents came from the northern flank during some high SSC events (Figure 3E).

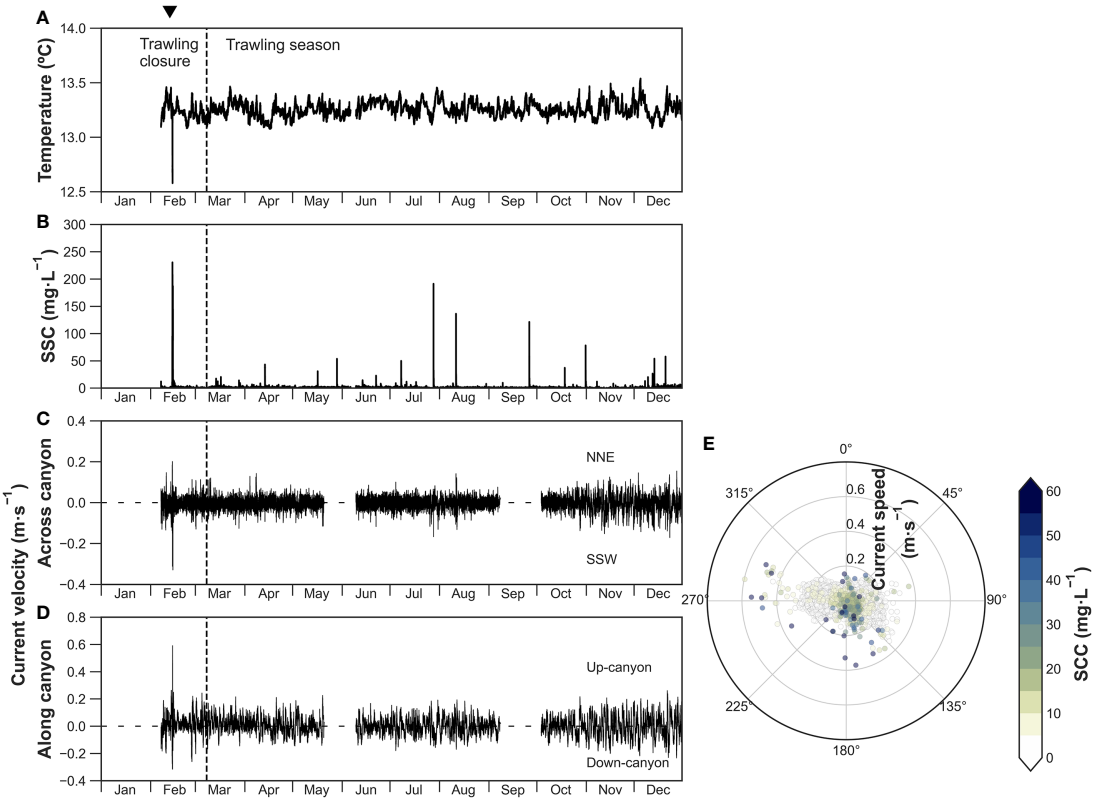

FIGURE 3
Axis-900 time-series of **(A)** temperature at 6 mab, **(B)** suspended sediment concentration (SSC), **(C)** across-canyon current velocity, and **(D)** along-canyon current velocity. **(E)** Polar plot of non-rotated current direction (angle), current speed (radius) and turbidity (color bar) at 5 mab. The inverted triangle on top indicates the occurrence of a dense shelf water cascading event. Note the different axis of along canyon and across canyon current speeds.

3.3 Sediment transport in the Montgrí tributary (975 m water depth)

In the Flank-1000 mooring located in the Montgrí tributary gully, temperatures at 5 mab fluctuated between 13.2 and 13.6°C during the whole sampling period, with no apparent change (Figure 4A). In contrast, recordings of SSC, current speed, and direction indicate frequent sediment transport events into the canyon's interior that follow a distinct temporal trend (Figures 4B-D). During the trawling closure in February, SSC was negligible at all depths, aside for a small near-bottom (5-10 mab) SSC peak of ~60 mg·L^{-1} as well as a sharp off-shore and down-flank increase in current speed of 0.4 m·s^{-1} and 0.2 m·s^{-1}, respectively, that occurred in coincidence with the eastern storm and DSWC event of mid-February (Figures 4B-D).

At the onset of the trawling period in March, peaks of near-bottom SSC (~400 mg·L^{-1}) and current speeds (~0.4 m·s^{-1}) caused by trawling-induced sediment gravity flows were recorded down-flank through the tributary (~190°; Figures 4B-D) on a daily basis, only during weekdays. The magnitude of these sediment transport events generally decreased throughout the year to SSC of ~50 mg·L^{-1} and were limited to between 5-20 mab (Figure 4B). Despite this general decreasing trend, exceptionally high sporadic near-bottom SSC of 250-770 mg·L^{-1} were observed in summer months that were accompanied with strong down-flank current speeds of between 0.25 m·s^{-1} to 0.6 m·s^{-1} (Figures 4C, D). Sediment gravity flows through the Montgrí tributary gully were absent in late October and throughout November when bottom trawlers moved to the open slope (Figure S2), but resumed again in December, with near-bottom SSC between 100 and 260 mg·L^{-1} and current speeds of ~0.2 m·s^{-1} (Figures 4B-D).

3.4 Sediment transport in canyon axis (1230 m water depth)

In the Axis-1200 mooring, temperature remained relatively constant, fluctuating between 13.1-13.4°C (Figure 5A) and did not present the sharp drop in temperature caused by the storm and DSWC event observed in the mooring further up-canyon

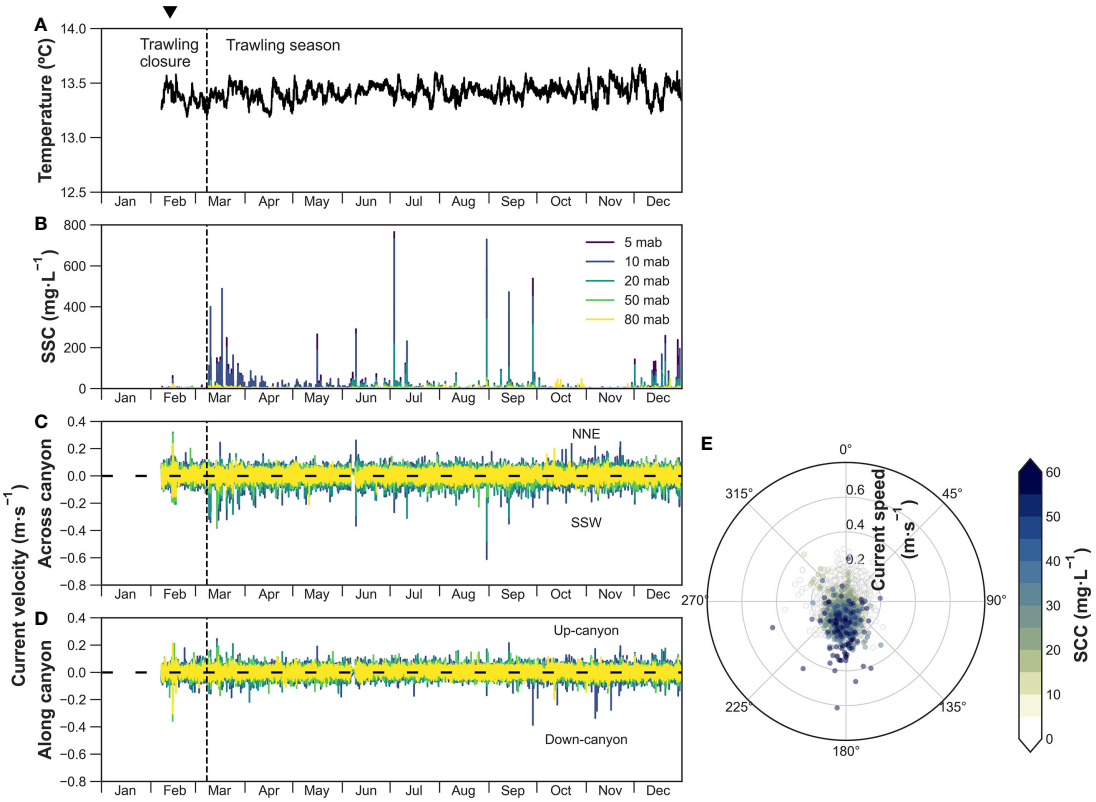

FIGURE 4
Flank-1000 time-series of **(A)** temperature at 5 mab, **(B)** suspended sediment concentration (SSC) at different water depths, **(C)** across-canyon current velocity at 10-80 mab, and **(D)** along-canyon current velocity at 10-80 mab. **(E)** Polar plot of non-rotated current direction (angle), current speed (radius) and turbidity (color bar) at 10 mab. The inverted triangle on top indicates the occurrence of a dense shelf water cascading event.

(Figure 3A). Instead, temperature presented a slight increase from 13.2 °C to 13.4 °C at the beginning of the event (Figure 5A) concurrent with an increase of near-bottom SSC >28.5 mg·L^{-1}, above the sensor range, and a peak of near-bottom current speed of 0.66 m·s^{-1} directed across-canyon and coming from the northern flank (Figures 5B, C). One day later, on February 15, a second peak of SSC >28.5 mg·L^{-1} was recorded, coinciding with another strong bottom current speed that reached 0.66 m·s^{-1} directed down-canyon (Figures 5B, D). A second sharp increase in SSC occurred on February 27, reaching the maximum turbidity reading values of >28.5 mg·L^{-1}, with strong across-canyon bottom current speed of 0.58 m·s^{-1} coming from the northern flank (Figures 5B, C). At the onset of bottom trawling in March, near-bottom SSC presented sharp increases of ~20 mg·L^{-1} only during weekdays (Figures 5A, B). Unfortunately, sensors in this first deployment stopped working on March 21.

During the second deployment in summer, frequent increases in SSC from ~1 mg·L^{-1} to between 60 and 230 mg·L^{-1} were recorded from June to early September, accompanied by increases in across-canyon current speed from 0.1 m·s^{-1} to 0.45 m·s^{-1} (Figures 5B–D). Some of these sediment gravity flows were directed towards the S and came from the Montgrí tributary gully (Figures 5C, E), occurring in coincidence to the sediment gravity flows recorded in the Flank-1000 mooring that had SSC exceeding 250 mg·L^{-1} (Figure 4). The remaining sediment gravity flows were directed towards the SSW and came from an adjacent tributary gully to the Montgrí, or towards the SE, coming from the upper canyon axis (Figure 5E). A strong sediment gravity flow was again registered in October 24, reaching high near-bottom SSC of 135 mg·L^{-1} coupled with strong down-canyon (0.25 m·s^{-1}) and NNW (0.15 m·s^{-1}) bottom currents (Figures 5B, D). Aside from the down-flank sediment gravity flows registered during the summer, the predominant bottom currents during the sampling period were essentially directed down-canyon (Figure 5E).

3.5 Downward particle fluxes and composition in canyon axis (1230 m water depth)

Downward TMF was highly variable during the whole sampling period, averaging 45.9 g·m^{-2}·d^{-1} but ranging from 7.4

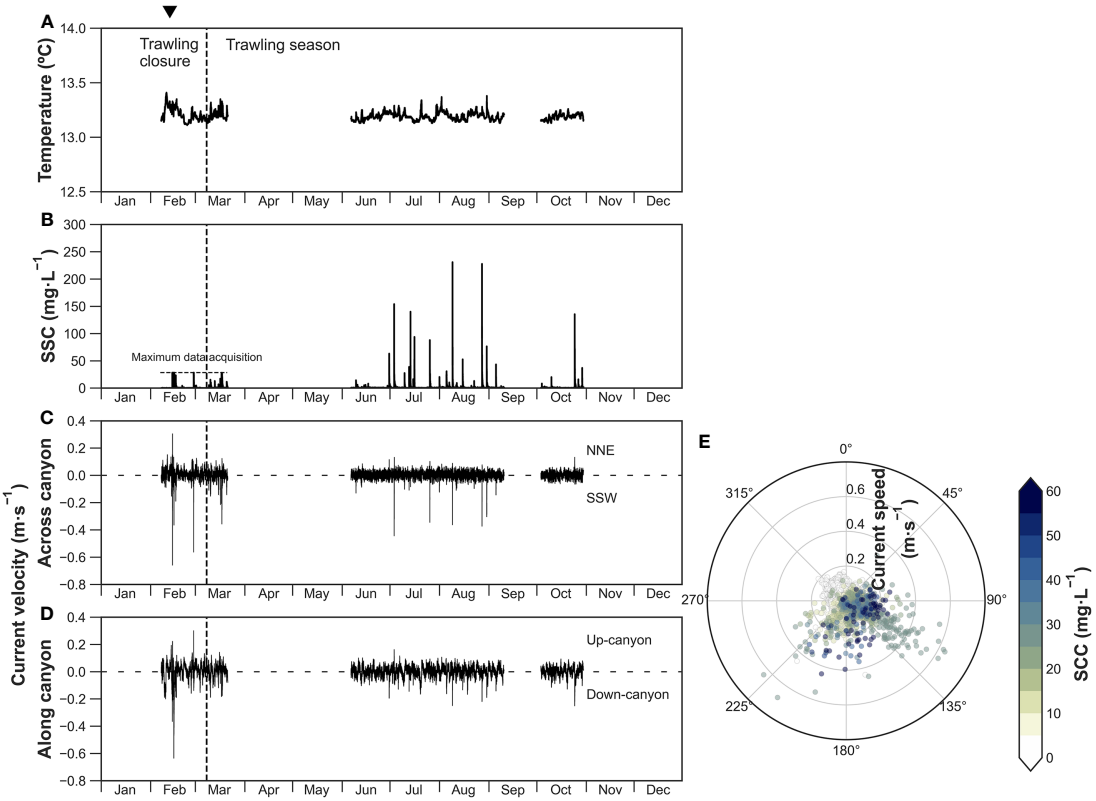

FIGURE 5
Axis-1200 time-series of **(A)** temperature, **(B)** suspended sediment concentration (SSC), **(C)** across-canyon current velocity, and **(D)** along-canyon current velocity. Note the maximum data acquisition for SSC in the first deployment. **(E)** Polar plot of non-rotated current direction (angle), current speed (radius) and turbidity (color bar) at 5 mab. The inverted triangle on top indicates the occurrence of a dense shelf water cascading event.

$g \cdot m^{-2} \cdot d^{-1}$ to >140 $g \cdot m^{-2} \cdot d^{-1}$ (Figure 6A). Due to the lack of data between March and June, a complete analysis of seasonal variability is not possible. At the beginning of the sampling period, TMF values increased from 29 $g \cdot m^{-2} \cdot d^{-1}$ in mid-February to >140 $g \cdot m^{-2} \cdot d^{-1}$ when the sediment trap overfilled in early March, at the onset of the bottom trawling season. Downward TMF presented sporadic increases from mid-June to late-September that ranged from approximately 50 $g \cdot m^{-2} \cdot d^{-1}$ to 125 $g \cdot m^{-2} \cdot d^{-1}$, which occurred in coincidence with sediment gravity flows coming from the northern flank (Figures 5A, 6A). Lower TMF values of approximately 14 $g \cdot m^{-2} \cdot d^{-1}$ were generally observed from October to early December, interrupted by a high TMF in late October (55 $g \cdot m^{-2} \cdot d^{-1}$) in coincidence with the sporadic sediment gravity flow coming from the southern canyon flank. The sediment trap overfilled in early December (>93 $g \cdot m^{-2} \cdot d^{-1}$), which resulted in an overfilled sample cup and the clogging of the sediment trap funnel.

The flux weighed average of the mean grain size was 12.8 μm during the whole sampling period, and ranged from 7.7 μm to 20.0 μm, generally following the patterns of TMF (Figure 6A). Sediment grain size consisted of mostly silt (71%) and clay (27%) fractions (Figure 6B), with slight increases in sand content from 0.5 to 6.5% during periods with highest TMF (> 40 $g \cdot m^{-2} \cdot d^{-1}$) (Figures 6A, B). The highest sand contents of 6.5% and 5.2% were detected in the overfilled sediment trap samples from March and December, respectively (Figure 6C). In comparison to surficial sediment from the adjacent trawled flank, sediment trap samples had finer grain size (Figures 6A, B). The predominant major constituents of the downward particle fluxes were lithogenic and $CaCO_3$ fractions with relatively constant values (average 70% and 26% respectively). Downward particle fluxes presented similar $CaCO_3$ contents as surficial sediment in the sediment core collected in the adjacent trawled site (Figure 6C).

The flux weighed mean of OC and TN contents was 0.91% and 0.11%, respectively, and followed a clear seasonal pattern with high contents at the beginning of the year (0.99% OC, 0.12% TN) that generally decreased in late-spring and summer to minimum values (0.86% OC, 0.10% TN), and increased again in autumn towards the end of the year (1.05% OC, 0.13% TN) (Figure 6D). The OC/TN molar ratio had a flux weighted mean of 8.2, and ranged from 7.2 to 10.2, with highest values occurring during high TMF in the summer (Figure 6E). Concentrations of OC and TN in the sediment trap samples during the winter months were 45 and 57% higher, respectively, than those quantified in the surficial sediment of the trawled sediment core, but presented similar values during the summer months (Figure 6D).

The composition of organic matter was investigated by calculating the OC-normalized contents of different types of biomarkers (in μg of biomarker per 100 mg of OC), which showed considerable variations throughout the sampling period (Figure 7). Terrestrial vanillyl phenols (VP) and syringyl phenols (SP) displayed low concentrations during the February storm and DSWC event (44 and 40 μg·100 mg^{-1} OC, respectively), but reached maximum concentrations in the overfilled sample in March at the beginning of the trawling season (65 and 50 μg·100 mg^{-1} OC, respectively), with values similar to those of the surface sediment from the adjacent trawled flank (Figure 7A). In contrast, terrigenous cinnamyl phenols (CP) and cutin acids (CA) presented relatively constant concentrations during this period (18 and 59 μg·100 mg^{-1} OC, respectively). During the summer, concentrations of terrestrial compounds were similar to those quantified in the surficial sediment of the core collected in the adjacent trawling flank, although small sporadic increases occurred in mid-July and early September (Figures 7A, B). Small increases in these compounds were also detected during the late-October sediment gravity flow, as well as the overfilled sediment trap in early-December. Ratios of SP/VP and CP/VP in the sediment trap ranged from 0.6 to 1.1 and from 0.2 to 0.4, respectively, whereas ratios of acid to aldehyde of vanillyl phenols (Vd/Vl) and syringyl phenols (Sd/Sl) ranged from 0.4 to 1.1 and from 0.2 to 0.8, respectively (Figure S3).

From the heterogenous compound classes, p-hydroxybenzenes (PB) and benzoic acids (BA) presented a similar pattern as VP and SP, with low concentrations during the February storm and DSWC event (31 and 9 μg·100 mg^{-1} OC, respectively) that peaked with the overfilling of the sediment trap in March (51 and 22 μg·100 mg^{-1} OC, respectively), reaching similar values as those from the surface sediment sampled in the adjacent trawled area (Figure 7C). Concentrations of PB and BA were initially high in early-summer (64 and 27 μg·100 mg^{-1} OC, respectively) and then decreased to similar values as those observed in the surficial sediment of the trawled site (Figure 7C). Towards the end of summer, concentrations of PB and BA increased again to 64 and 22 μg·100 mg^{-1} OC, respectively, but dropped to 35 and 8 μg·100 mg^{-1} OC, respectively, during the late-October sediment gravity flow (Figure 7C).

The fatty acid (FA), dicarboxylic acid (DA) and amino acid (AA) CuO products are highly enriched in marine organic matter sources (e.g., phytoplankton, zooplankton) relative to terrestrial plants (Goñi and Hedges, 1995). Given their high degradability, these compounds are rapidly transformed during their transport towards the seafloor, so presence of these compounds in downward particulate fluxes generally indicate the arrival of fresh marine organic matter, often derived from periods of high net primary productivity (Goni et al., 2009). These compounds presented higher OC-normalized concentrations during the mid-February eastern storm and DSWC event (89, 65 and 568 μg·100 mg^{-1} OC) and decreased during the following weeks (72, 52 and 390 μg·100 mg^{-1} OC) (Figures 7D, E). However, concentrations increased again in the overfilled sediment trap in March. The summer months generally presented lower concentrations (~55, ~40 and ~245 μg·100 mg^{-1} OC, respectively), similar to the surficial

sediment of the core collected in the trawled flank. Exceptionally high concentrations (103, 78 and 621 μg·100 mg^{-1} OC) were observed in early June, as observed with PB and BA, as well as in mid-July and mid-September. Concentrations remained low and similar to the surface sediment of the trawled area during the remaining sampling period, with another increase in concentration in the overfilled sediment trap in early December (68, 39 and 380 μg·100 mg^{-1} OC) (Figures 7D, E).

The variations in OC composition in downward particulate fluxes are summarized in a PCA, which in total explained 74% of the variance (Figure 8). Eigenvalue scores show that higher PC1 values reflect greater concentrations of all CuO compounds, consistent with the presence of organic matter with higher overall biomarker abundances, whereas different groups of CuO compounds are differentiated along the PC2 axis in terms of their general reactivity, as observed by Paradis et al. (2021b) (Figure 8A). With the exception of the last sediment

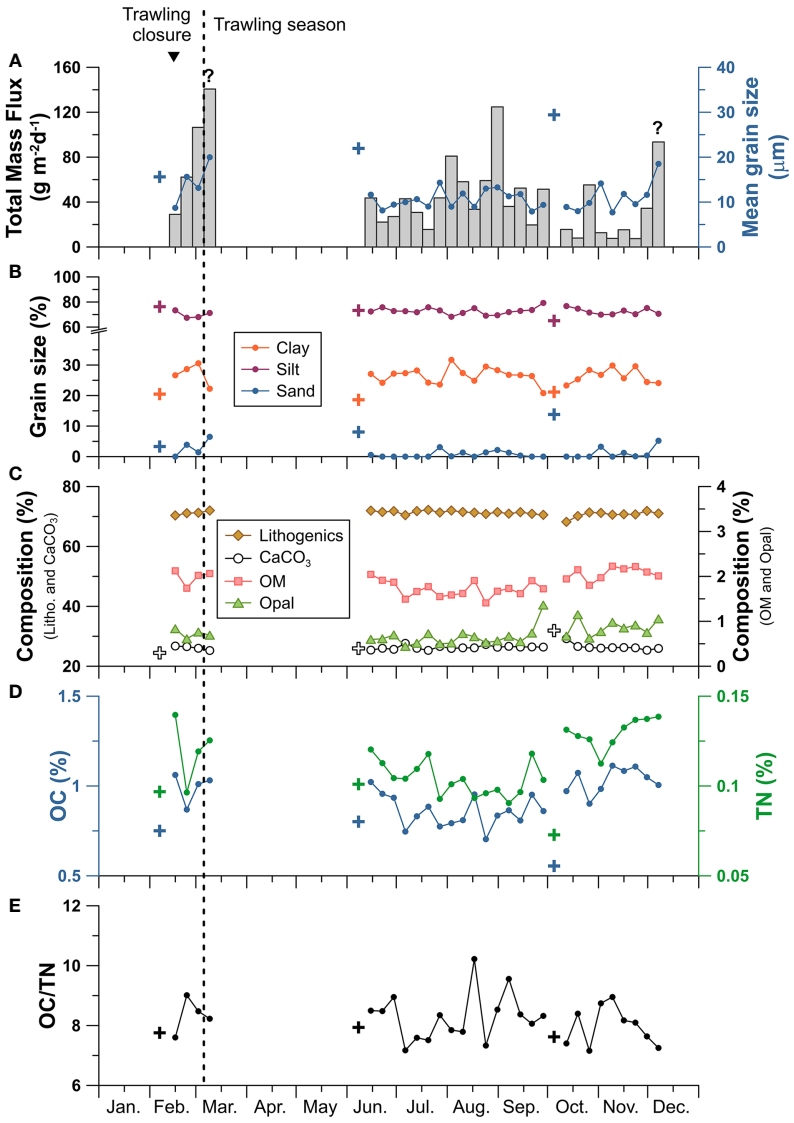

FIGURE 6
Axis-1200 time series of the sediment trap: **(A)** total mass flux (TMF) in grey bars and mean grain size in blue circles, **(B)** grain size classes, **(C)** relative concentration of the main mass composition: lithogenics (brown diamonds), calcium carbonate ($CaCO_3$, white circles), organic matter (OM, pink squares), and biogenic opal (green triangles), **(D)** organic carbon (OC) in blue and total nitrogen (TN) in green, and **(E)** OC/TN molar ratio. Question marks above TMF bars indicate that the sediment trap had overfilled in that sample and the inverted triangle indicates the occurrence of a dense shelf water cascading event. Mean values of grain size, $CaCO_3$, OC, and TN of surficial sediment of the sediment core retrieved on the trawled flank in February, June, and October (Paradis et al., 2021b) are given with crosses. Note the break in the axis of the grain size fraction **(B)**.

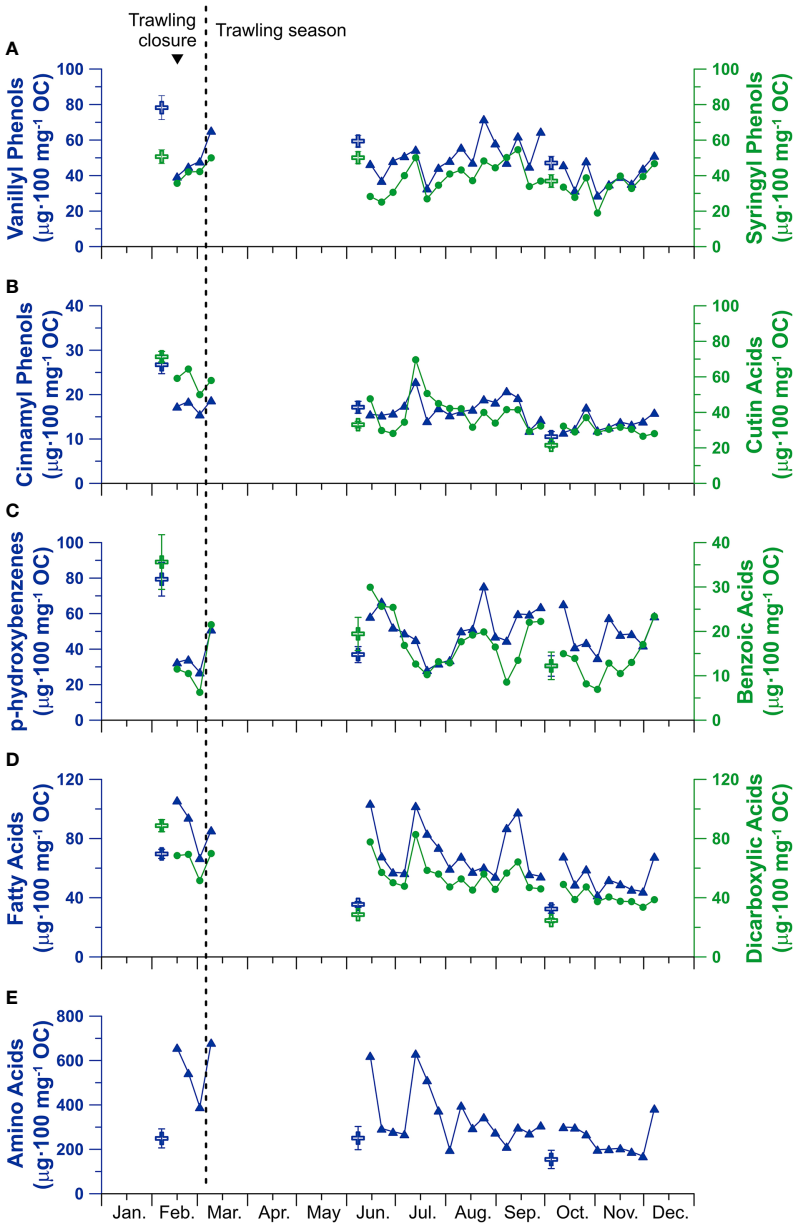

FIGURE 7
Temporal evolution of OC-normalized CuO compound classes in the sediment trap samples (Axis-1200). **(A)** terrestrial vanillyl (blue triangles) and syringyl (green circles) phenols, **(B)** terrestrial cinnamyl phenols (blue triangles) and cutin acids (green circles), **(C)** p-hydroxy benzenes (blue triangles) and benzoic acids (green circles), **(D)** fatty acids (blue triangles) and di-carboxylic acids (green circles), **(E)** amino acids (blue triangles). Values of surficial sediment of the sediment core retrieved on the trawled flank in February, June, and October (Paradis et al., 2021b) are given with crosses. Note the different scales for each compound classes. The inverted triangle on top indicates the occurrence of a dense shelf water cascading event.

trap sample from early-March, the temporal evolution of PC1 generally reflects higher values during the trawling closure than during the trawling season (Figure 8B). In contrast, during the trawling season, higher TMF values are normally associated to lower PC1 and PC2 values, similar to values of surficial samples from the adjacent trawling ground (Figures 8B, C).

4 Discussion

During the 2017 sampling period, several sediment transport events of both natural and anthropic origin were identified in Palamós Canyon. Storms occurred during winter and autumn months, characteristic of seasonal patterns of this margin

(Palanques et al., 2005; Zúñiga et al., 2009; Lopez-Fernandez et al., 2013b) with exceptionally strong eastern storms in mid-January and mid-February (Figures 2A, B). These natural forcing conditions abated during the spring and summer months, when bottom trawling activities were predominant in the surroundings of Palamós Canyon (Figure 2; Palanques et al., 2006; Puig et al., 2012; Martín et al., 2014a). Both storms and trawling activities transported sediment into the canyon through different pathways and with different sediment composition. The following sections describe and discuss in detail each of these events chronologically.

4.1 Winter storm and dense shelf water cascading (February)

An exceptionally strong eastern storm occurred a week prior to the mooring deployment in mid-January, causing a flash flood of the Ter River (Figures 2A, B). This flood event transported terrestrial organic matter to the margin and reached the northern flank of Palamós Canyon (Figure 1), which we sampled two weeks after this storm. The surface sediment recovered from this core had high concentrations of lignin phenols and cutin acids from vascular plants, reflecting fresh terrestrial inputs from the storm (Figures 7A, B; Paradis et al., 2021b).

This storm was followed by another eastern storm a week after the deployment of the moorings in mid-February that drove the cascading of dense shelf water into the upper Palamós Canyon axis, reaching the Axis-900 mooring, which registered a drop in temperatures (< 12.6°C), as well as an increase in turbidity (~230 mg·L^{-1}) and current speed (0.6 m·s^{-1}) (Figures 3A, B; Arjona-Camas et al., 2021). No drop of temperatures was observed either in Flank-1000 nor in Axis-1200, the latter mooring located ~4 km down-canyon from Axis-900, indicating that these dense waters had reached neutral buoyancy at shallower depths. However, this DSWC event prompted the transport of suspended sediment through the entire canyon. The Flank-1000 mooring registered SSC of ~50 mg·L^{-1} and current speeds of 0.4 m s^{-1}, while the Axis-1200 mooring registered SSC >28.5 mg·L^{-1} and current speeds of 0.6 m s^{-1} (Figure S4). However, the turbidimeter at Axis-1200 recorded maximum values during that event due to the sensor range limitation (28.5 mg·L^{-1}), and we expect that actual SSC were significantly higher given the simultaneous increases in SSC in all moorings (Figure S4).

The strong sediment transport event associated to DSWC in the Axis-1200 mooring did not lead to high downward sediment fluxes in the sediment trap (Figure 6A), which could indicate either a stronger horizontal rather than vertical sediment flux that would have bypassed the sediment trap, or that the sediment transport occurred close to the seafloor and was missed by the sediment trap located at 22 mab, as hypothesized in other studies (Bonnin et al., 2008; Rumín-Caparrós et al., 2016). Moreover, high current speeds can affect sediment trap collection efficiency (Baker et al., 1988; Heussner et al., 2006), so downward particulate fluxes during this event should be considered as semi-quantitative.

Downward sediment fluxes from the mid-February eastern storm and DSWC event had higher concentrations of OC and TN (1.1% and 0.14%, respectively) (Figure 6D) enriched in compound classes of marine origin (i.e. fatty acids,

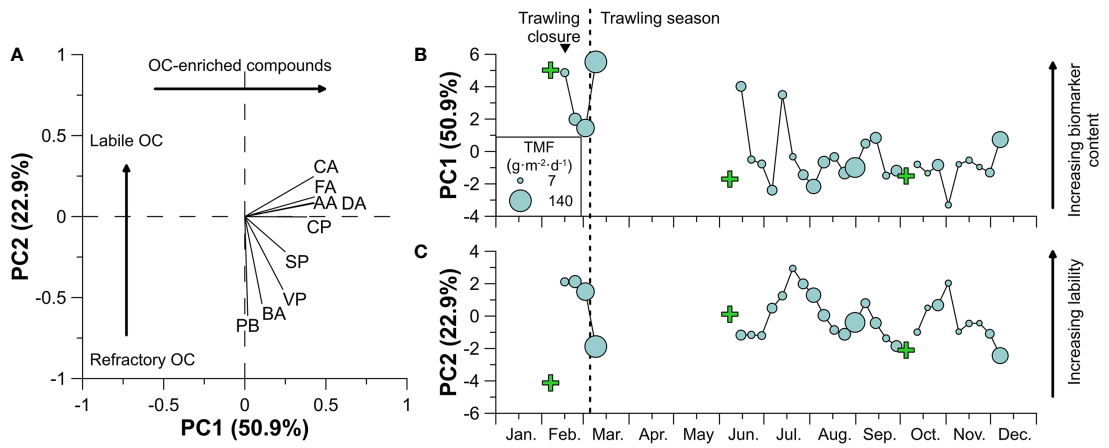

FIGURE 8
PCA results. **(A)** Eigenvalues of the PCA performed of OC-normalized CuO products in the sediment trap (Axis-1200). Temporal evolution of **(B)** PC1 and **(C)** PC2 values of the sediment trap samples, where the size of the circles refers to TMF and the green crosses show the PC value of surficial sediment of the sediment core retrieved on the trawled flank in February, June, and October (Paradis et al., 2021b). The inverted triangle on top indicates the occurrence of a dense shelf water cascading event.

dicarboxylic acids, and amino acids) (Figures 7D, E) in comparison to particulate matter accumulated during the following week (Figure S4). This peak in marine biomarkers coincided with elevated estimates of NPP that were consistent with a winter phytoplankton bloom. Although this storm caused high Ter River discharge (Figure 2B) that reached off-shore sediments on the Palamós northern flank (Paradis et al., 2021b), the organic matter in the sediment traps had low OC-normalized concentrations of terrestrial compounds because they were diluted by the enhanced contribution of fresh marine organic compounds from the phytoplankton bloom (Figure 2). Other studies have shown similar trends, where the usual transfer of OC-poor terrigenous organic matter into canyons during storms (Tesi et al., 2010; Sanchez-Vidal et al., 2012) is offset by the transfer of fresh marine organic matter during phytoplankton blooms (Fabres et al., 2008; Pasqual et al., 2010; Lopez-Fernandez et al., 2013a). Hence, these high-energy DSWC events can result in important drivers of fresh and labile organic matter from surface shelf and slope waters to deep-sea environments, while also transferring fluvial derived terrestrial material.

During the following 2 weeks, downward sediment fluxes in the sediment trap increased from ~30 to ~100 $g{\cdot}m^{-2}{\cdot}d^{-1}$ (Figure 6A), indicating the settling of sediment that had remained in suspension after the DSWC event (Arjona-Camas et al., 2021). These samples displayed lower OC and TN contents and decreasing OC-normalized concentrations of the most labile compounds (i.e. amino acids, fatty acids, dicarboxylic acids; Figures 7, 8), which indicate the resuspension and transfer of OC-poor sediment resuspended by the strong DSWC currents (Puig et al., 2008). Alternatively, these trends could also reflect a general degradation of these compounds given their long transit time in the water column before reaching the sediment trap.

4.2 Onset of trawling season (March)

Bottom trawling activities began on March 8, after 2 months of a trawling closure on the fishing grounds surrounding Palamós Canyon (BOE, 2017). At the onset of bottom trawling activities, high sediment fluxes were recorded at the Axis-900 mooring (Arjona-Camas et al., 2021), and sediment gravity flows with high SSC (200-400 $mg{\cdot}L^{-1}$) and strong bottom currents (~0.4 $m{\cdot}s^{-1}$) were channeled through the Montgrí tributary gully, recorded by the Flank-1000 mooring, some reaching the Axis-1200 mooring ~1.5 km further down-flank (Figure S5). The strong sediment gravity flows occurring on Thursday and Friday (March 10 and 11) that reached Axis-1200 with SSC between 10-20 $mg{\cdot}L^{-1}$ would have caused the overfilling of that week's sediment trap cup, with a total mass flux of >140 $g{\cdot}m^{-2}{\cdot}d^{-1}$ (Figure S5). Sediment transported at the onset of the trawling season had coarser grain size with higher sand content than the previous trap samples (Figures 6B, S5), as observed in trawling-induced sediment gravity flows from a sediment trap deployed in this same site in 2002 (Palanques et al., 2006).

Downward sediment flux during the onset of the trawling season was enriched in most biomarkers, including terrestrial compounds (lignin phenols) and labile marine compounds (fatty acids, di-carboxylic acids, and amino acids) in comparison to the previous trap sample (Figures 7, S5), with a similar overall composition to surficial sediment from the trawled flank (Figure 8; Paradis et al., 2021b). This confirms that bottom trawling is translocating sediment from the fishing grounds into the canyon. The higher terrestrial content was associated to the transfer of surficial sediment from the fishing ground which was enriched in these compounds due to the Ter River flash flood that occurred in January (Paradis et al., 2021b), while the higher marine compounds indicate the transferal of the remnants of the phytoplankton bloom (see section 4.1).

4.3 Trawling season (March-October)

Previous studies observed that bottom trawling during the summer causes almost-daily sediment gravity flows through the Montgrí tributary only during working days (Palanques et al., 2006; Puig et al., 2012; Martín et al., 2014a), which were also evident during this study (Figures S5, S6). The intensity of these sediment gravity flows in Flank-1000 mooring decreased as the trawling season unfolded, from ~500 $mg{\cdot}L^{-1}$ in early March to ~15 $mg{\cdot}L^{-1}$ in late October, although some large isolated peaks were still registered (Figure 4A). This decreasing trend proves a progressive depletion of sediment available for resuspension by bottom trawling gears during the trawling season, as hypothesized in previous studies (Martín et al., 2014a).

Although these sediment gravity flows were directed towards the canyon axis, only the exceptionally intense sediment gravity flows (SSC >250 $mg{\cdot}L^{-1}$) at Flank-1000 reached the Axis-1200 mooring, causing SSC and TMF to increase from ~1 to 60-230 $mg{\cdot}L^{-1}$ and from ~16 to 120 $g{\cdot}m^{-2}{\cdot}d^{-1}$ respectively (Figure S6), with similar magnitude as those registered during the summer months at the same site in 2001 (Martín et al., 2006). These sediment gravity flows mainly originated from the Montgrí tributary gully (~190°), but also from an adjacent tributary gully towards the NNE (~220°) (Figure S6), as hypothesized in previous studies (Martín et al., 2006; Palanques et al., 2006). This proves that the various tributary gullies along the flanks of Palamós Canyon (Lastras et al., 2011) would likely serve as pathways of resuspended sediment from the fishing grounds along the canyon flanks into the canyon axis (Figure 1), presumably leading to increases in sedimentation rates not only at 1750 m in depth, as reported in previous studies (Martín et al., 2008; Puig et al., 2015), but likely throughout the whole canyon axis, as observed in the adjacent Blanes Canyon (Paradis et al., 2018b).

Trawling-derived sediment gravity flows transported coarser grain sizes in comparison to periods with naturally low TMFs (Figure S6), as observed by Palanques et al. (2006). However,

downward particulate matter collected by the sediment trap had finer grain size than surface sediment of trawling grounds (Figures 7A, B) as a result of grain size sorting and winnowing of finer grained sediment by bottom trawling (Martín et al., 2014b; Paradis et al., 2021b). The flux weighed mean concentration of OC and TN during this period (March-October) was lower (0.84% OC, 0.10% TN) than during the rest of the study period (1.00% OC, 0.13% TN) (Figures 6D, S6), which also coincided with the periods with lower net primary productivity in the area (Figure 2C). This could indicate that marine productivity is the main driver increasing OC and TN contents sinking to the seafloor, where submarine canyons play an important role in its transfer to deeper environments (Fabres et al., 2008; Lopez-Fernandez et al., 2013a; Grinyó et al., 2017), and that bottom trawling does not alter the OC and TN content of the downward particulate matter fluxes. However, the composition of OC obtained from CuO oxidation indicates that periods with high downward particulate fluxes due to bottom trawling-derived sediment gravity flows transferred highly degraded terrestrial compounds and lower content of the most labile marine compound classes, and its biogeochemical composition was similar to surficial sediment from the adjacent trawling ground (Figures 8, S6). Despite the similar biogeochemical composition to the trawled site, in the majority of the samples, OC, TN and the most labile compound classes (i.e. fatty acids, di-carboxylic acids, and amino acids) had slightly higher content in the sediment trap than in the trawling ground (Figures 6, 7), which reveals that the downward particle flux consisted of a combination of eroded sediment transferred from fishing grounds with hemipelagic settling of particulate organic matter enriched in biomarkers of marine origin (Figure 7). In contrast, in the absence of trawling-derived sediment gravity flows during the summer, particulate organic matter had higher content of reactive marine compound classes, such as in early June, associated to the high NPP occurring then (Figures 2C, 7).

4.4 Intermission of trawling activities (November-December)

Throughout October and November, SSCs in all three moorings were negligible, while the downward sediment fluxes in the sediment trap were only ~10 $g{\cdot}m^{-2}{\cdot}d^{-1}$ (Figures 3-6) with the exception of an isolated sediment gravity flow in late-October (Figure S7). This reduced sediment flux occurred in the absence of fishing activities in the Sant Sebastià fishing ground (Figure S2), confirming the strong relationship between sediment transport into Palamós Canyon and this anthropogenic activity. During this low sediment flux period, sediment collected in the Axis-1200 trap had higher OC and TN contents (1.04% OC, 0.13% TN), than during the summer months (0.84% OC, 0.10% TN) when frequent trawling-derived sediment gravity flows were registered in the canyon axis (Figures 6D, S7). This was likely the result of increasing NPP (Figure 2C) and the lower dilution of organic matter due to lower lithogenic transport during this period in comparison to periods with trawling-derived sediment gravity flows. This is supported by the more labile organic matter during this period (Figures 7, S7), indicating the transferal of fresh material into the canyon in the absence of trawling activities.

An isolated late-October sediment gravity flow coming from the southern flank interrupted the low TMF during the absence of trawling activities, which led to high TMF of ~60 $g{\cdot}m^{-2}{\cdot}d^{-1}$ with high lithogenic fraction that diluted the OC contents (Figure S7). In contrast to trawling-derived sediment gravity flows coming from the northern flank (see section 4.3), organic matter presented higher lability (Figure 8C), indicating the transferal of fresh material, albeit diluted by the high lithogenic fraction, into the canyon. Therefore, this sporadic sediment gravity flow seems to be associated to a natural sediment destabilization from the untrawled southern canyon flank, as previously observed in deeper parts of this canyon (Martín et al., 2006; 2007).

After five weeks of trawling intermission in Sant Sebastià fishing ground, bottom trawlers resumed their activity in December (Figure S2), increasing near-bottom SSCs to 130-260 $mg{\cdot}L^{-1}$ in Flank-1000 and to ~50 $mg{\cdot}L^{-1}$ in Axis-900 during that month, while the sediment trap in Axis-1200 overfilled once more, attaining a TMF of at least 94 $g{\cdot}m^{-2}{\cdot}d^{-1}$ (Figure S8). This increase in sediment transport in all moorings confirm that the fishing ground was replenished with new erodible sediment during the fishing intermittence, generating large sediment gravity flows when trawling activities resumed, as was observed at the onset of trawling season in early March (see section 4.2). In both overfilled trap samples, the sediment transported into the canyon consisted of coarser particles with high terrigenous and marine OC (Figures 6-8, S8), indicating the translocation of freshly-deposited sediment with higher organic matter contents into the canyon. This corroborates that chronic trawling disturbance depletes organic matter from fishing grounds (Pusceddu et al., 2014), while short periods without trawling disturbance are insufficient to allow its recovery (Paradis et al., 2021b), which swiftly remove the most OC-rich surficial sediment from fishing grounds when trawling activities resume.

4.5 Annual sediment transport and composition in Palamós Canyon

Sediment transport into Palamós Canyon during 2017 was highly dynamic, dominated by natural high-energy events such as eastern storms and DSWC, as well as by bottom trawling, both of which transferred large volumes of sediment into the canyon. Sediment transport through the Montgrí tributary gully was dominated by trawling-induced sediment gravity flows, which accounted for ~1500 $kg{\cdot}m^{-2}$ sediment whereas the eastern storm

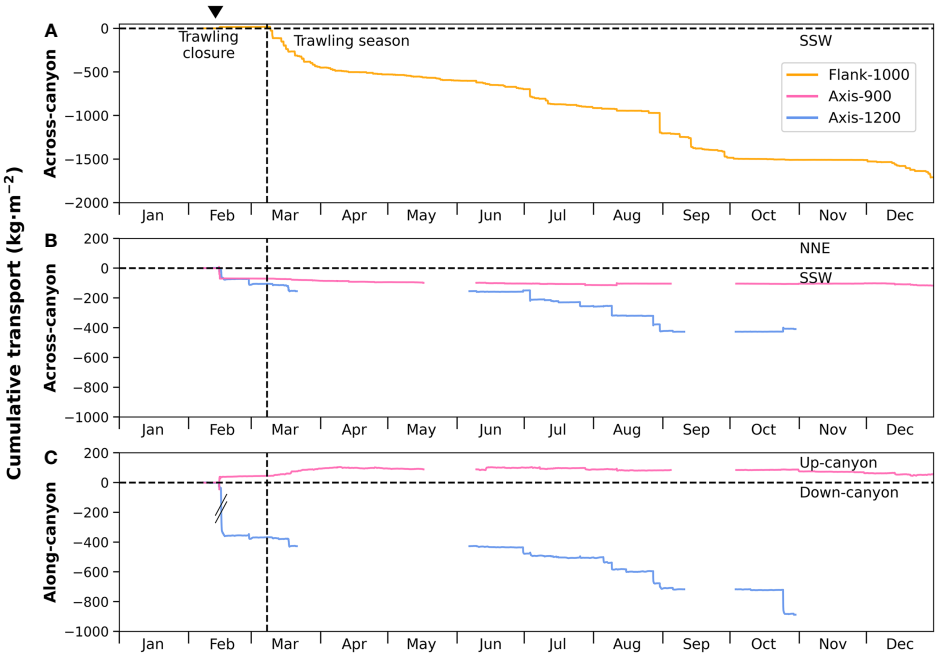

FIGURE 9
Time series of cumulative sediment transport at all moorings: **(A)** at the Flank-1000 mooring in the across-canyon direction (10 mab), **(B)** at Axis-900 and Axis-1200 in the across-canyon direction (5 mab) and **(C)** in the along-canyon direction (5 mab). Cumulative sediment transport for Axis-900 and Axis-1200 are highly underestimated due to their incomplete timeseries and the maximum data acquisition of the Axis-1200 turbidimeter during the first deployment (Figure 5). Note the different axes for the Flank-1000 cumulative sediment transport in comparison to the across-canyon and along-canyon transport of Axis-900 and Axis-1200. The inverted triangle on top indicates the occurrence of a dense shelf water cascading event.

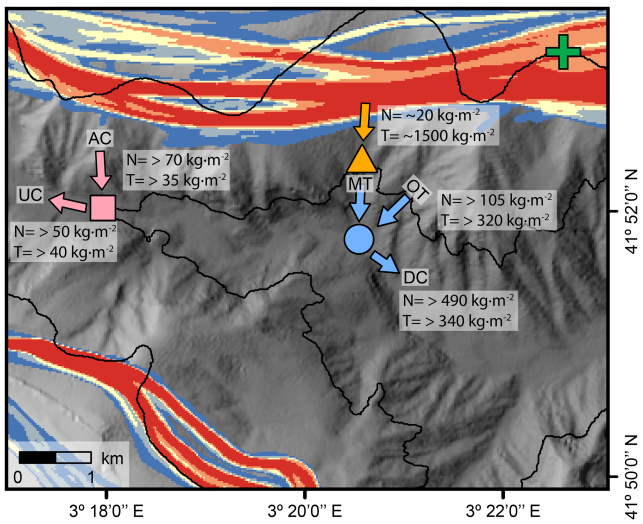

FIGURE 10
Map of main sediment transport pathways of the three mooring locations in Palamós Canyon: up-canyon (UC) and across-canyon (AC) for Axis-900 mooring (pink square), Montgrí tributary gully (MT) for Flank-900 mooring (orange triangle), other tributary gully (OT), and down-canyon (DC) for Axis-1200 mooring (blue circle). Annotated in the figure is the cumulative sediment transport for natural high-energy events (N) and trawling-derived events (T). Note that the across-canyon cumulative transport for the Axis-1200 mooring combines sediment transported through both tributaries (MT and OT).

and DSWC at the beginning of the year transported ~20 kg·m^{-2} of sediment through this tributary and into the canyon (Figures 9, 10). In the case of the moorings located along the canyon axis (Axis-900, Axis-1200), the magnitudes of sediment fluxes from natural and anthropogenic events were comparable (Figures 9, 10). In Axis-900, total sediment flux from storms and DSWC was at least ~120 kg·m^{-2} during 2017, while bottom trawling accounted for at least ~75 kg·m^{-2}. Further down-canyon, natural high-energy events transported at least ~600 kg·m^{-2} of sediment through Axis-1200 whereas trawling activities accounted for at least ~680 kg·m^{-2} of sediment (Figures 9, 10). Despite the comparable magnitude of sediment fluxes, natural events tend to be sporadic and seasonal, whereas bottom trawling causes continuous and persistent sediment fluxes into the canyon.

With regards to the composition of sediment transported into the canyon, it is worth noting that terrestrial compounds (i.e. lignin phenols and cutin acids) were detected during the whole sampling period (Figure 7), irrespectively of the sediment transport process, as observed in other submarine canyons nearby (Tesi et al., 2010; Pasqual et al., 2013), which confirms the role of submarine canyons as across-margin conduits of terrestrial organic matter towards deep-sea basins. The high acid to aldehyde ratio of vanillyl and syringyl phenols, SP/VP and CP/VP ratios (Figure S3) indicates that terrestrial organic matter was highly degraded and mostly originated from non-woody angiosperm leaves and grasses (Hedges and Mann, 1979; Goñi and Hedges, 1995). The highly degraded compositions are expected given the distance of the Axis-1200 mooring to the shore and the long transit times that promote its alteration (Pasqual et al., 2013). Presence of non-woody organic matter signatures is also expected given the association of these compounds to fine-grained sediment that can be more easily transported offshore than larger-sized woody detritus with high vanillyl phenol contents, which tend to accumulate in more nearshore environments (Gordon and Goñi, 2004; Pasqual et al., 2013; Zhang et al., 2014).

Bottom trawling-derived sediment fluxes in the canyon axis had lower OC content (~0.8%) and consisted of more degraded organic matter in comparison to downward sediment fluxes in the absence of bottom trawling during the summer, as well as in comparison to the sediment fluxes during the storms in February (~1% OC), since these natural processes occurred in coincidence with high net primary productivity in surface waters or an intermittence of fishing activities. The enhanced particulate matter fluxes of eroded sediment by bottom trawling modify the OC composition of downward particulate fluxes in submarine canyons from fresh marine organic matter to degraded and less reactive terrestrial organic matter. This alteration in the nutritional value of organic matter would affect the benthic community structure inhabiting submarine canyons, and could explain the lower diversity of meiofauna mainly consisting of opportunistic nematode species as observed within the axes of the studied canyon (Pusceddu et al., 2014) as well as in the adjacent Blanes Canyon (Román et al., 2018).

Despite the lower OC content of these trawling-derived sediment fluxes (~0.8%), the higher TMF associated to bottom trawling activities (>54 kg·m^{-2}; Figure 6A), indicate that a substantial amount of organic carbon is transferred into the canyon (> 0.43 kg OC·m^{-2}), where it will eventually be buried in the canyon axis. Since efficient OC burial is generally associated to high sedimentation rates (Blair and Aller, 2012; Bianchi et al., 2018), the enhanced sediment transfer and resulting increase in sedimentation rates in the canyon axis by bottom trawling activities (Martín et al., 2008; Puig et al., 2015) could lead to high OC burial in the canyon axis. However, this enhanced transport of OC by bottom trawling activities could partially offset the OC lost from fishing grounds (Martín et al., 2014b; Paradis et al., 2021b), and further studies will be necessary to properly quantify the sediment and the OC budgets in Palamós Canyon, and assess the potential effects on benthic communities.

5 Conclusion

High energy events such as river floods and storms are important mechanisms that enhance the transport of particulate matter into submarine canyons, but recent studies have emphasized that bottom trawling activities modify natural sedimentary dynamics within these geomorphological features. This study shows how bottom trawling is altering sedimentary dynamics in submarine canyons and reveals that the organic matter composition of down-canyon particulate matter is modified by this anthropogenic activity. While winter storms transport terrigenous and fresh marine organic matter into the canyon in the presence of phytoplankton blooms, trawling-induced sediment gravity flows transfer more degraded organic matter. Trawling events interrupt the naturally high concentrations of fresh and reactive organic matter compounds that are usually transferred during the calm summer months, which could affect benthic communities that inhabit the canyon and rely on the input of fresh organic matter. However, the higher downward particulate fluxes into the canyon by bottom trawling also increases organic carbon fluxes, urging to better constrain the sediment and organic carbon budgets in bottom trawling-affected submarine canyons.

Data availability statement

The raw data supporting the conclusions of this article will be made available by the authors, without undue reservation.

Author contributions

SP, MA-C, AP, and PP conceptualized the study design and performed the fieldwork. MA-C and SP analyzed sensor data from moorings. SP performed the laboratory analyses and interpreted the

results alongside MG. AP, PM, and PP provided funding for the study. SP wrote the manuscript with the contribution of all co-authors, who approve the submitted version.

Funding

The results presented in this study were obtained within the "Assessment of Bottom-trawling Impacts in Deep-sea Sediments" (ABIDES) Spanish Research Project (CTM2015-65142-R). Additional funds were provided by the Generalitat de Catalunya (2017 SGR-663 and SGR- 1588), by the Australian Research Council LIEF Project (LE170100219) and by the "Assessment of Bottom-trawling Resuspension Impacts in deep benthic Communities" (ABRIC) Spanish Research Project (RTI2018-096434-B-I00). This work is contributing to the ICTA's "Unit of Excellence" Maria de Maetzu (CEX2019-000940-M), and ICM-CSIC's "Center of Excellence" Severo Ochoa (CEX2019-000928-S). Open access funding provided by ETH Zurich.

Acknowledgments

We would like to thank the crew of the R/V García del Cid as well as Elena Martinez, Neus Maestro, and Silvia de Diago, who helped collect and process the samples. The IAEA is grateful for the support provided to its Environment Laboratories by the Government of the Principality of Monaco.

Conflict of interest

The authors declare that the research was conducted in the absence of any commercial or financial relationships that could be construed as a potential conflict of interest.

Publisher's note

All claims expressed in this article are solely those of the authors and do not necessarily represent those of their affiliated organizations, or those of the publisher, the editors and the reviewers. Any product that may be evaluated in this article, or claim that may be made by its manufacturer, is not guaranteed or endorsed by the publisher.

Supplementary material

The Supplementary Material for this article can be found online at: https://www.frontiersin.org/articles/10.3389/fmars.2022.1017052/full#supplementary-material

References

Allen, S. E., and Durrieu de Madron, X. (2009). A review of the role of submarine canyons in deep-ocean exchange with the shelf. *Ocean Sci.* 5, 607–620. doi: 10.5194/os-5-607-2009

Arjona-Camas, M., Puig, P., Palanques, A., Durán, R., White, M., Paradis, S., et al. (2021). Natural vs. trawling-induced water turbidity and sediment transport variability within the palamós canyon (NW Mediterranean). *Mar. Geophys. Res.* 42, 38. doi: 10.1007/s11001-021-09457-7

Arjona-Camas, M., Puig, P., Palanques, A., Emelianov, M., and Durán, R. (2019). Evidence of trawling-induced resuspension events in the generation of nepheloid layers in the foix submarine canyon (NW Mediterranean). *J. Mar. Syst.* 196, 86–96. doi: 10.1016/j.jmarsys.2019.05.003

Baker, E. T., Milburn, H. B., and Tennant, D. A. (1988). Field assessment of sediment trap efficiency under varying flow conditions. *J. Mar. Res.* 46, 573–592. doi: 10.1357/002224088785113522

Behrenfeld, M. J., and Falkowski, P. G. (1997). Photosynthetic rates derived from satellite-based chlorophyll concentration. *Limnol. Oceanogr.* 42, 1–20. doi: 10.4319/lo.1997.42.1.0001

Bianchi, T. S., Cui, X., Blair, N. E., Burdige, D. J., Eglinton, T. I., and Galy, V. (2018). Centers of organic carbon burial and oxidation at the land-ocean interface. *Org. Geochem.* 115, 138–155. doi: 10.1016/j.orggeochem.2017.09.008

Bjørkan, M., Company, J. B., Gorelli, G., Sardà, F., and Massaguer, C. (2020). *When fishemen take charge: The development of a management plan for the red shrimp fishery in Mediterranean Sea (NE Spain)* (Cham: Springer), 159–178. doi: 10.1007/978-3-030-26784-1_10

Blair, N. E., and Aller, R. C. (2012). The fate of terrestrial organic carbon in the marine environment. *Ann. Rev. Mar. Sci.* 4, 401–423. doi: 10.1146/annurev-marine-120709-142717

BOE (2017). Resolución de 26 de enero de 2017, de la secretaría general de pesca, por la que se fija, para 2017, el periodo de veda establecido en la orden AAA/923/2013, de 16 de mayo, por la que se regula la pesca de gamba rosada (Aristeus antennatus) con arte de arrastre de fondo en determinadas zonas marítimas próximas a palamós. *Boletin Oficial del Estado* 30, 8169.

Bonnin, J., Heussner, S., Calafat, A., Fabres, J., Palanques, A., Durrieu de Madron, X., et al. (2008). Comparison of horizontal and downward particle fluxes across canyons of the gulf of lions (NW mediterranean): Meteorological and hydrodynamical forcing. *Cont. Shelf Res.* 28, 1957–1970. doi: 10.1016/j.csr.2008.06.004

Canals, M., Puig, P., de Madron, X. D., Heussner, S., Palanques, A., and Fabres, J. (2006). Flushing submarine canyons. *Nature* 444, 354. doi: 10.1038/nature05271

Daly, E., Johnson, M. P., Wilson, A. M., Gerritsen, H. D., Kiriakoulakis, K., Allcock, A. L., et al. (2018). Bottom trawling at whittard canyon: Evidence for seabed modification, trawl plumes and food source heterogeneity. *Prog. Oceanogr.* 169, 227–240. doi: 10.1016/j.pocean.2017.12.010

De Leo, F. C., Vetter, E. W., Smith, C. R., Rowden, A. A., and McGranaghan, M. (2014). Spatial scale-dependent habitat heterogeneity influences submarine canyon macrofaunal abundance and diversity off the main and Northwest Hawaiian islands. *Deep Sea Res. Part II Top. Stud. Oceanogr.* 104, 267–290. doi: 10.1016/j.dsr2.2013.06.015

de Stigter, H. C., Boer, W., de Jesus Mendes, P. A., Jesus, C. C., Thomsen, L., van den Bergh, G. D., et al. (2007). Recent sediment transport and deposition in the nazaré canyon, Portuguese continental margin. *Mar. Geol.* 246, 144–164. doi: 10.1016/j.margeo.2007.04.011

Durrieu de Madron, X., Ferré, B., Le Corre, G., Grenz, C., Conan, P., Pujo-Pay, M., et al. (2005). Trawling-induced resuspension and dispersal of muddy sediments and dissolved elements in the gulf of lion (NW Mediterranean). *Cont. shelf Res.* 25 (19-20), 2387–2409. doi: 10.1016/j.pocean.2004.08.004

Fabres, J., Tesi, T., Velez, J., Batista, F., Lee, C., Calafat, A., et al. (2008). Seasonal and event-controlled export of organic matter from the shelf towards the gulf of lions continental slope. *Cont. Shelf Res.* 28, 1971–1983. doi: 10.1016/j.csr.2008.04.010

Farrugio, H. (2012). "A refugium for the spawners of exploited Mediterranean marine species: the canyons of the continental slope of the gulf of lion," in *Mediterranean Submarine canyons: Ecology and governance*. Ed. M. Würtz (Gland, Switzerland: International Union for Conservation of Nature), 45–50.

Fernandez-Arcaya, U., Ramirez-Llodra, E., Aguzzi, J., Allcock, A. L., Davies, J. S., Dissanayake, A., et al. (2017). Ecological role of submarine canyons and need for canyon conservation: A review. *Front. Mar. Sci.* 4. doi: 10.3389/fmars.2017.00005

Goni, M. A., Aceves, H., Benitez-Nelson, B., Tappa, E., Thunell, R., Black, D. E., et al. (2009). Oceanographic and climatologic controls on the compositions and fluxes of biogenic materials in the water column and sediments of the cariaco basin over the late Holocene. *Deep Sea Res. Part I Oceanogr. Res. Pap.* 56, 614–640. doi: 10.1016/j.dsr.2008.11.010

Goñi, M. A., and Hedges, J. I. (1995). Sources and reactivities of marine-derived organic matter in coastal sediments as determined by alkaline CuO oxidation. *Geochim. Cosmochim. Acta* 59, 2965–2981. doi: 10.1016/0016-7037(95)00188-3

Goñi, M. A., and Montgomery, S. (2000). Alkaline CuO oxidation with a microwave digestion system: Lignin analyses of geochemical samples. *Anal. Chem.* 72, 3116–3121. doi: 10.1021/ac991316w

Goñi, M. A., O'Connor, A. E., Kuzyk, Z. Z., Yunker, M. B., Gobeil, C., and Macdonald, R. W. (2013). Distribution and sources of organic matter in surface marine sediments across the north American Arctic margin. *J. Geophys. Res. Ocean.* 118, 4017–4035. doi: 10.1002/jgrc.20286

Gordon, E. S., and Goñi, M. A. (2004). Controls on the distribution and accumulation of terrigenous organic matter in sediments from the Mississippi and atchafalaya river margin. *Mar. Chem.* 92, 331–352. doi: 10.1016/J.MARCHEM.2004.06.035

Grinyó, J., Isla, E., Peral, L., and Gili, J.-M. (2017). Composition and temporal variability of particle fluxes in an insular canyon of the northwestern Mediterranean Sea. *Prog. Oceanogr.* 159, 323–339. doi: 10.1016/j.pocean.2017.11.005

Hedges, J. I., and Mann, D. C. (1979). The characterization of plant tissues by their lignin oxidation products. *Geochim. Cosmochim. Acta* 43, 1803–1807. doi: 10.1016/0016-7037(79)90028-0

Heussner, S., Durrieu de Madron, X., Calafat, A., Canals, M., Carbonne, J., Delsaut, N., et al. (2006). Spatial and temporal variability of downward particle fluxes on a continental slope: Lessons from an 8-yr experiment in the gulf of lions (NW Mediterranean). *Mar. Geol.* 234, 63–92. doi: 10.1016/J.MARGEO.2006.09.003

Heussner, S., Ratti, C., and Carbonne, J. (1990). The PPS 3 time-series sediment trap and the trap sample processing techniques used during the ECOMARGE experiment. *Continent. Shelf Res.* 10, 943–958. doi: 10.1016/0278-4343(90)90069-X

Hsu, R. T., Liu, J. T., Su, C.-C., Kao, S.-J., Chen, S.-N., Kuo, F.-H., et al. (2014). On the links between a river's hyperpycnal plume and marine benthic nepheloid layer in the wake of a typhoon. *Prog. Oceanogr.* 127, 62–73. doi: 10.1016/j.pocean.2014.06.001

Lastras, G., Canals, M., Amblas, D., Lavoie, C., Church, I., De Mol, B., et al. (2011). Understanding sediment dynamics of two large submarine valleys from seafloor data: Blanes and la fonera canyons, northwestern Mediterranean Sea. *Mar. Geol.* 280, 20–39. doi: 10.1016/j.margeo.2010.11.005

Liu, J. T., Wang, Y.-H., Yang, R. J., Hsu, R. T., Kao, S.-J., Lin, H.-L., et al. (2012). Cyclone-induced hyperpycnal turbidity currents in a submarine canyon. *J. Geophys. Res. Ocean.* 117, C04033. doi: 10.1029/2011JC007630

Lopez-Fernandez, P., Bianchelli, S., Pusceddu, A., Calafat, A., Sanchez-Vidal, A., and Danovaro, R. (2013a). Bioavailability of sinking organic matter in the blanes canyon and the adjacent open slope (NW Mediterranean Sea). *Biogeosciences* 10, 3405–3420. doi: 10.5194/bg-10-3405-2013

Lopez-Fernandez, P., Calafat, A., Sanchez-Vidal, A., Canals, M., Mar Flexas, M., Cateura, J., et al. (2013b). Multiple drivers of particle fluxes in the blanes submarine canyon and southern open slope: Results of a year round experiment. *Prog. Oceanogr.* 118, 95–107. doi: 10.1016/j.pocean.2013.07.029

Martín, J., Palanques, A., and Puig, P. (2006). Composition and variability of downward particulate matter fluxes in the palamós submarine canyon (NW Mediterranean). *J. Mar. Syst.* 60, 75–97. doi: 10.1016/j.jmarsys.2005.09.010

Martín, J., Palanques, A., and Puig, P. (2007). Near-bottom horizontal transfer of particulate matter in the palamós submarine canyon (NW Mediterranean). *J. Mar. Res.* 65, 193–218. doi: 10.1357/002224007780882569

Martín, J., Palanques, A., Vitorino, J., Oliveira, A., and de Stigter, H. C. (2011). Near-bottom particulate matter dynamics in the nazaré submarine canyon under calm and stormy conditions. *Deep Sea Res. Part II Top. Stud. Oceanogr.* 58, 2388–2400. doi: 10.1016/j.dsr2.2011.04.004

Martín, J., Puig, P., Masqué, P., Palanques, A., and Sánchez-Gómez, A. (2014a). Impact of bottom trawling on deep-sea sediment properties along the flanks of a submarine canyon. *PloS One* 9, e104536. doi: 10.1371/journal.pone.0104536

Martín, J., Puig, P., Palanques, A., Masqué, P., and García-Orellana, J. (2008). Effect of commercial trawling on the deep sedimentation in a Mediterranean submarine canyon. *Mar. Geol.* 252, 150–155. doi: 10.1016/j.margeo.2008.03.012

Martín, J., Puig, P., Palanques, A., and Ribó, M. (2014b). Trawling-induced daily sediment resuspension in the flank of a Mediterranean submarine canyon. *Deep Sea Res. Part II Top. Stud. Oceanogr.* 104, 174–183. doi: 10.1016/j.dsr2.2013.05.036

Mendoza, E. T., and Jiménez, A. A. (2009). "Vulnerability assessment to coastal storms at a regional scale," in *Coastal engineering 2008*, vol. vol 5. , 4154–4166.

Mortlock, R. A., and Froelich, P. N. (1989). A simple method for the rapid determination of biogenic opal in pelagic marine sediments. *Deep Sea Res. Part A. Oceanogr. Res. Pap.* 36, 1415–1426. doi: 10.1016/0198-0149(89)90092-7

Nieuwenhuize, J., Maas, Y. E. M., and Middelburg, J. J. (1994). Rapid analysis of organic carbon and nitrogen in particulate materials. *Mar. Chem.* 45, 217–224. doi: 10.1016/0304-4203(94)90005-1

Palanques, A., García-Ladona, E., Gomis, D., Martín, J., Marcos, M., Pascual, A., et al. (2005). General patterns of circulation, sediment fluxes and ecology of the palamós (La fonera) submarine canyon, northwestern Mediterranean. *Prog. Oceanogr.* 66, 89–119. doi: 10.1016/j.pocean.2004.07.016

Palanques, A., Martín, J., Puig, P., Guillén, J., Company, J. B., and Sardà, F. (2006). Evidence of sediment gravity flows induced by trawling in the palamós (Fonera) submarine canyon (northwestern Mediterranean). *Deep Sea Res. Part I Oceanogr. Res. Pap.* 53, 201–214. doi: 10.1016/j.dsr.2005.10.003

Palanques, A., and Puig, P. (2018). Particle fluxes induced by benthic storms during the 2012 dense shelf water cascading and open sea convection period in the northwestern Mediterranean basin. *Mar. Geol.* 406, 119–131. doi: 10.1016/j.margeo.2018.09.010

Palanques, A., Puig, P., Durrieu de Madron, X., Sanchez-Vidal, A., Pasqual, C., Martín, J., et al. (2012). Sediment transport to the deep canyons and open-slope of the western gulf of lions during the 2006 intense cascading and open-sea convection period. *Prog. Oceanogr.* 106, 1–15. doi: 10.1016/j.pocean.2012.05.002

Paradis, S., Goñi, M., Masqué, P., Durán, R., Arjona-Camas, M., Palanques, A., et al. (2021b). Persistence of biogeochemical alterations of deep-Sea sediments by bottom trawling. *Geophys. Res. Lett.* 48, e2020GL091279. doi: 10.1029/2020GL091279

Paradis, S., lo Iacono, C., Masqué, P., Puig, P., Palanques, A., Russo, T., et al. (2021a). Evidence of large increases in sedimentation rates due to fish trawling in submarine canyons of the gulf of Palermo (SW Mediterranean). *Mar. pollut. Bull.* 172, 112861. doi: 10.1016/j.marpolbul.2021.112861

Paradis, S., Masqué, P., Puig, P., Juan-Díaz, X., Gorelli, G., Company, J. B., et al. (2018a). Enhancement of sedimentation rates in the foix canyon after the renewal of trawling fleets in the early XXIst century. *Deep Res. Part I Oceanogr. Res. Pap.* 132, 51–59. doi: 10.1016/j.dsr.2018.01.002

Paradis, S., Puig, P., Masqué, P., and Juan-Díaz, X. (2017). Bottom-trawling along submarine canyons impacts deep sedimentary regimes. *Sci. Rep.* 7, 43332. doi: 10.1038/srep43332

Paradis, S., Puig, P., Sánchez-Vidal, A., Masqué, P., García-Orellana, J., Calafat, A., et al. (2018b). Spatial distribution of sedimentation-rate increases in blanes canyon caused by technification of bottom trawling fleet. *Prog. Oceanogr.* 169, 241–252. doi: 10.1016/j.dsr.2018.01.002

Pasqual, C., Goñi, M.A., Tesi, T., Sanchez-Vidal, A., Calafat, A., and Canals, M. (2013). Composition and provenance of terrigenous organic matter transported along submarine canyons in the gulf of lion (NW Mediterranean Sea). *Prog. Oceanogr.* 118, 81–94. doi: 10.1016/j.pocean.2013.07.013

Pasqual, C., Sanchez-Vidal, A., Zúñiga, D., Calafat, A., Canals, M., Durrieu de Madron, X., et al. (2010). Flux and composition of settling particles across the continental margin of the gulf of lion: the role of dense shelf water cascading. *Biogeosciences* 7, 217–231. doi: 10.5194/bg-7-217-2010

Pedregosa, F., Varoquaux, G., Gramfort, A., Michel, V., Thirion, B., Grisel, O., et al. (2011). Scikit-learn: Machine learning in Python. *J. Mach. Learn. Res.* 12, 2825–2830.

Pedrosa-Pàmies, R., Sanchez-Vidal, A., Calafat, A., Canals, M., and Durán, R. (2013). Impact of storm-induced remobilization on grain size distribution and organic carbon content in sediments from the blanes canyon area, NW Mediterranean Sea. *Prog. Oceanogr.* 118, 122–136. doi: 10.1016/j.pocean.2013.07.023

Porter, M., Inall, M. E., Hopkins, J., Palmer, M. R., Dale, A. C., Aleynik, D., et al. (2016). Glider observations of enhanced deep water upwelling at a shelf break canyon: A mechanism for cross-slope carbon and nutrient exchange. *J. Geophys. Res. Ocean.* 121, 7575–7588. doi: 10.1002/2016JC012087

Puig, P., Canals, M., Company, J. B., Martín, J., Amblas, D., Lastras, G., et al. (2012). Ploughing the deep sea floor. *Nature* 489, 286–289. doi: 10.1038/nature11410

Puig, P., Martín, J., Masqué, P., and Palanques, A. (2015). Increasing sediment accumulation rates in la fonera (Palamós) submarine canyon axis and their relationship with bottom trawling activities. *Geophys. Res. Lett.* 42, 8106–8113. doi: 10.1002/2015GL065052

Puig, P., Palanques, A., and Martín, J. (2014). Contemporary sediment-transport processes in submarine canyons. *Ann. Rev. Mar. Sci.* 6, 53–77. doi: 10.1146/annurev-marine-010213-135037

Puig, P., Palanques, A., Orange, D. L., Lastras, G., and Canals, M. (2008). Dense shelf water cascades and sedimentary furrow formation in the cap de creus canyon, northwestern Mediterranean Sea. *Cont. Shelf Res.* 28 (15), 2017–2030. doi: 10.1016/j.csr.2008.05.002

Pusceddu, A., Bianchelli, S., and Danovaro, R. (2015). Quantity and biochemical composition of particulate organic matter in a highly trawled area (Thermaikos gulf, Eastern Mediterranean Sea). *Adv. Oceanogr. Limnol.* 6, 21–32. doi: 10.4081/aiol.2015.5448

Pusceddu, A., Bianchelli, S., Martin, J., Puig, P., Palanques, A., Masque, P., et al. (2014). Chronic and intensive bottom trawling impairs deep-sea biodiversity and ecosystem functioning. *Proc. Natl. Acad. Sci.* 111, 8861–8866. doi: 10.1073/pnas.1405454111

Ribó, M., Puig, P., Palanques, A., and Lo Iacono, C. (2011). Dense shelf water cascades in the cap de creus and palamós submarine canyons during winters 2007 and 2008. *Mar. Geol.* 284, 175–188. doi: 10.1016/j.margeo.2011.04.001

Román, S., Vanreusel, A., Ingels, J., and Martin, D. (2018). Nematode community zonation in response to environmental drivers in blanes canyon (NW Mediterranean). *J. Exp. Mar. Bio. Ecol* 502, 111–128. doi: 10.1016/j.jembe.2017.08.010

Rumín-Caparrós, A., Sanchez-Vidal, A., González-Pola, C., Lastras, G., Calafat, A., and Canals, M. (2016). Particle fluxes and their drivers in the avilés submarine canyon and adjacent slope, central cantabrian margin, bay of Biscay. *Prog. Oceanogr.* 144, 39–61. doi: 10.1016/j.pocean.2016.03.004

Sanchez-Vidal, A., Canals, M., Calafat, A. M., Lastras, G., Pedrosa-Pàmies, R., Menéndez, M., et al. (2012). Impacts on the deep-Sea ecosystem by a severe coastal storm. *PloS One* 7, e30395. doi: 10.1371/journal.pone.0030395

Sanchez-Vidal, A., Pasqual, C., Kerhervé, P., Calafat, A., Heussner, S., Palanques, A., et al. (2008). Impact of dense shelf water cascading on the transfer of organic matter to the deep western Mediterranean basin. *Geophys. Res. Lett.* 35, L05605. doi: 10.1029/2007GL032825

Sardà, F., Cartes, J. E., and Norbis, W. (1994). Spatio-temporal structure of the deep-water shrimp aristeus antennatus (Decapoda: Aristeidae) population in the western Mediterranean. *Fish. Bull.* 92, 599–607.

Sparkes, R. B., Lin, I.-T., Hovius, N., Galy, A., Liu, J. T., Xu, X., et al. (2015). Redistribution of multi-phase particulate organic carbon in a marine shelf and canyon system during an exceptional river flood: Effects of typhoon morakot on the gaoping river–canyon system. *Mar. Geol.* 363, 191–201. doi: 10.1016/J.MARGEO.2015.02.013

Tesi, T., Langone, L., Goñi, M. A., Turchetto, M., Miserocchi, S., and Boldrin, A. (2008). Source and composition of organic matter in the bari canyon (Italy): Dense water cascading versus particulate export from the upper ocean. *Deep Sea Res. Part I Oceanogr. Res. Pap.* 55, 813–831. doi: 10.1016/j.dsr.2008.03.007

Tesi, T., Puig, P., Palanques, A., and Goñi, M. A. (2010). Lateral advection of organic matter in cascading-dominated submarine canyons. *Prog. Oceanogr.* 84, 185–203. doi: 10.1016/J.POCEAN.2009.10.004

Tudela, S., Sardà, F., Maynou, F., and Demestre, M. (2003). Influence of submarine canyons on the distribution of the deep-water shrimp, *Aristeus antennatus* (Risso 1816) in the NW Mediterranean. *Crustaceana* 76, 217–225. doi: 10.1163/156854003321824567

Vetter, E. W., Smith, C. R., and De Leo, F. C. (2010). Hawaiian Hotspots: Enhanced megafaunal abundance and diversity in submarine canyons on the oceanic islands of Hawaii. *Mar. Ecol.* 31, 183–199. doi: 10.1111/j.1439-0485.2009.00351.x

Wilson, A. M., Kiriakoulakis, K., Raine, R., Gerritsen, H. D., Blackbird, S., Allcock, A. L., et al. (2015). Anthropogenic influence on sediment transport in the whittard canyon, NE Atlantic. *Mar. pollut. Bull.* 101, 320–329. doi: 10.1016/j.marpolbul.2015.10.067

Wu, Y., Liu, Z., Hu, J., Zhu, Z., Liu, S., and Zhang, J. (2016). Seasonal dynamics of particulate organic matter in the changjiang estuary and adjacent coastal waters illustrated by amino acid enantiomers. *J. Mar. Syst.* 154, 57–65. doi: 10.1016/j.jmarsys.2015.04.006

Zhang, Y., Kaiser, K., Li, L., Zhang, D., Ran, Y., and Benner, R. (2014). Sources, distributions, and early diagenesis of sedimentary organic matter in the pearl river region of the south China Sea. *Mar. Chem.* 158, 39–48. doi: 10.1016/j.marchem.2013.11.003

Zúñiga, D., Flexas, M. M., Sanchez-Vidal, A., Coenjaerts, J., Calafat, A., Jordà, G., et al. (2009). Particle fluxes dynamics in blanes submarine canyon (Northwestern Mediterranean). *Prog. Oceanogr.* 82, 239–251. doi: 10.1016/j.pocean.2009.07.002